2010-10-08

Effects of Thermal Gradient and Fines Content on Frost Heave of an Alaska Base Material

Adam Ray Homewood
Brigham Young University - Provo

Effects of Thermal Gradient and Fines Content on Frost Heave of an Alaska Base Material

Adam R. Homewood

A thesis submitted to the faculty of
Brigham Young University
in partial fulfillment of the requirements for the degree of

Master of Science

W. Spencer Guthrie, Chair
Gustavious P. Williams
Paul W. Richards

Department of Civil and Environmental Engineering

Brigham Young University

December 2010

ABSTRACT

Effects of Thermal Gradient and Fines Content on Frost Heave of an

Alaska Base Material

Adam R. Homewood

Department of Civil and Environmental Engineering

Master of Science

The objective of this research was to investigate the effects of thermal gradient and fines content and the interaction between these two factors on the frost heave characteristics of a typical Alaska base material. The laboratory frost heave testing involved one type of aggregate base material, three thermal gradients, and three fines contents in a full-factorial experimental design with two replicates. The aggregate was classified in the American Association of State Highway and Transportation Officials soil classification system as A-1-a; the thermal gradients were 0.15, 0.30, and 0.45 ºC/cm; and the fines contents were 6, 8, and 10 percent.

After frost heave testing, a stepwise regression analysis was performed to identify significant independent variables for each of nine separate dependent variables, including frost heave, heave-uptake ratio, steady-state frost heave rate, gravimetric water ingress, and gravimetric water content in each of the five individual lifts tested following frost heave testing. Soil suction, specific gravity, salinity, and hydraulic conductivity testing were also performed on samples prepared at each of the three fines contents to support numerical modeling of the frost heave test results using the computer program ICE-1.

The results of the stepwise regression analysis indicate that thermal gradient is a significant predictor of six of the nine dependent variables and that the square of thermal gradient is a significant predictor of five of these six dependent variables. As the thermal gradient increased, the samples experienced decreasing amounts of water ingress and frost heave. However, the data show that neither fines content nor the square of fines content is a significant predictor of any of the dependent variables. Thus, although previous research has shown that higher fines contents are generally associated with greater susceptibility to frost heave, this effect is not manifest in the comparatively small increases in fines contents evaluated in this research. The interaction between thermal gradient and fines content is a significant predictor of only one independent variable. Differences between the modeled and measured frost heave values ranged from 0.01 to 0.92 cm, with the larger differences typically associated with the lowest thermal gradient and the lowest fines content.

Keywords: aggregate base material, base course, fines content, freezing, frost heave, frost susceptibility, hydraulic conductivity, matric suction, osmotic suction, thermal gradient

ACKNOWLEDGMENTS

The author thanks and acknowledges Dr. W. Spencer Guthrie for his constant enthusiasm and guidance through the duration of this project. The author acknowledges Dr. Xiong Zhang and Dr. Jenny Liu for providing the funding and material that made this research possible. The author thanks Rodney Mayo for his expertise in running the test equipment, as well as all the research assistants who took part in this research project. Finally, the author thanks his wonderful wife, Sarah Homewood, for her support, encouragement, and love.

TABLE OF CONTENTS

LIST OF TABLES

LIST OF FIGURES

1 INTRODUCTION

1.1 Problem Statement

Understanding the mechanics of frost heave is important because it has the potential to cause catastrophic damage to roads, pipelines, bridges, and structures. Cold-region engineers have had difficulty in attaching a price tag to the damages incurred due to heaving pressures on roadways and other structures; however, government transportation engineers working in cold regions have estimated that at least half of road maintenance costs are due to freezing and thawing (*1*). The high costs of repair and reconstruction have caught the attention of many cold regions researchers and engineers, who have investigated frost heaving in order to better understand the process and how it can be mitigated (*2, 3, 4, 5, 6, 7, 8, 9*). Researchers have found that, in order for frost heave to occur, three elements must be present: sustained freezing temperatures, an available water source, and a frost-susceptible material (*10, 11*).

Freezing temperatures are usually defined as those below 0°C. However, in nature, the point at which individual water molecules reorient themselves into a crystalline lattice structure is often found to be several degrees below 0°C. The freezing-point depression occurs because extra energy must be removed to “freeze out” any ions present in the water; through this ion exclusion process, ice crystals form from water in a pure deionized state (*12, 13*). For this reason, saline solutions can remain unfrozen at subfreezing temperatures (*14*). Another way in which the freezing temperature of soil water is lowered is the adsorption of water molecules to mineral surfaces. The majority of the soil particles comprising base and subgrade materials

possess a negative surface charge, which electrically attracts the positive ends of individual water molecules and binds them to the mineral surface (*15*). Although the intensity of the electrical attraction diminishes exponentially with increasing distance from the mineral surface (*15*), the effects of adsorption can prevent bound water molecules from being incorporated into ice; this effect becomes less pronounced with lower temperatures as the bonds are de-energized.

Water in freezing soil systems can be supplied from several sources, including precipitation, underground aquifers, and manmade features, for example. During winter, when heat is removed from the ground surface such that frost penetration begins, a vertical temperature gradient is created due to the warmer temperatures of the earth's subsurface layers. Through the development of cryosuction in the upper soil strata, water is drawn upwards toward the freezing front. As the ice crystals grow, they force the soil particles apart and become a continuous layer of nearly pure ice (*16*). The growth of these ice lenses causes the ground to heave upward.

The susceptibility of a soil to frost heave is commonly determined by the individual grain sizes of the soil particles. Relatively large particles, such as those found in sands and gravels, do not have the ability to develop high magnitudes of cryosuction due to the relatively large amount of pore space that typically exists between the particles. Clays, on the other hand, have the potential to develop significant cryosuction but usually exhibit such low hydraulic conductivity that the occurrence of frost heave is greatly restricted. For these reasons, gravels, sands, and clays are not considered to be highly frost-susceptible. Silts, though, consisting of intermediate grain sizes able to both develop high levels of cryosuction and allow water flow, are highly frost-susceptible (*17*). Because performing actual frost heave tests, either in the laboratory or in the field, requires specialized equipment, frost-susceptibility ratings are often determined from soil classifications (*7*); a widely used method developed by the United States Army Corps of

Engineers classifies soils into four groups labeled F1 through F4, with F4 being the most susceptible to frost heave (*18*).

To limit frost heave of pavement structures, personnel at the Alaska Department of Transportation (AKDOT), in particular, specify a maximum of 6 percent finer than the 0.075-mm sieve for aggregate base materials to be used in construction of Alaska highways. As high-quality aggregate is not readily available in many parts of Alaska, however, AKDOT engineers have become interested in revising the materials specifications to permit the statewide use of lesser-quality aggregates containing more fines. While previous research has shown that higher fines contents are generally associated with greater susceptibility to frost heave (*7, 19, 20, 21, 22*), the effects of comparatively small increases in fines contents on frost heave behavior typical of Alaska base materials has not been investigated.

Because Alaska is so geographically distributed, a variety of thermal gradients exist at different locations in the state. While previous research has addressed the effect of fines content on frost heave, the interaction between thermal gradient and fines content has not been specifically investigated. Knowing if the effect of fines depends upon the magnitude of thermal gradient is essential for AKDOT engineers considering applications of new specifications statewide. Therefore, the purpose of this research was to investigate the effects of thermal gradient and fines content and the interaction between these two factors on the frost heave characteristics of a typical Alaska base material. The project was completed by Brigham Young University (BYU) research personnel in partnership with researchers at the University of Alaska at Fairbanks (UAF).

1.2 Scope

The laboratory frost heave testing associated with this research involved one type of aggregate base material, three thermal gradients, and three fines contents. Two replicate specimens were created for each unique combination, yielding a total of 18 test specimens. The material used for this project was classified by the American Association of State Highway and Transportation Officials (AASHTO) classification system as an A-1-a granular soil. This material was sampled from Fairbanks, Alaska, and was supplied by UAF research personnel. Supplementary fines were also supplied from Fairbanks and were added to each of the 18 samples to achieve fines contents, defined as the percentage by mass finer than the 0.075 mm sieve, of 6, 8, and 10 percent. Three thermal gradients, including 0.15, 0.30, and 0.45 ºC/cm, were selected to represent different geographic regions of Alaska. The results of this research project are only applicable to the specific soil type, thermal gradients, and fines contents investigated in this research.

1.3 Outline of Report

This report contains five chapters. Chapter 1 explains the objectives of this research along with the scope and outline of the project. Chapter 2 presents a detailed description of the physical mechanisms and damage potential of frost heave. Chapter 3 describes the procedures performed for each experiment. Chapter 4 presents the results of the frost heave experiments, and Chapter 5 provides a detailed summary of the research findings together with recommendations for further research.

2 BACKGROUND

2.1 Overview

The following sections present information gathered through the literature review conducted for this research. Specifically, descriptions of frost heave mechanisms and frost heave damage are given.

2.2 Frost Heave Mechanisms

Frost heave is a phenomenon that has been studied for over 80 years, beginning with the experiments of G. J. Bouyoucos, the soil physicist, who ascertained that pore water in soils will not uniformly crystallize at the same temperature (*23*). Bouyoucos's research lead to further significant advances in the understanding of frost heave from the seminal papers of S. Taber (*24, 25, 26*). Taber rejected the hypothesis that frost heave in soil was caused solely by the expansion of water as it crystallized and proposed a new theory involving ice lenses that is widely accepted today; G. Beskow's detailed monograph on the mechanism of frost heave strengthened and expanded Taber's original work (*27*).

As the atmospheric temperature falls below freezing, ice begins to nucleate within the pore water. Nucleation of ice cannot take place without some kind of crystal nuclei on which the ice can first form. Examples of crystal nuclei are dust particles and air bubbles. Starting in the center of the pore space and gradually expanding outwards, ice begins filling the pores. When water changes from a liquid to a solid state, it increases in volume by 9 percent. This expansion

is known as primary heave, and, due to the small increase in volume, the corresponding heave pressure is also relatively small (*28*).

As pore water turns into ice, the soil becomes increasingly devoid of liquid water. This desiccation creates suction forces that cause available water to attempt to move up through the soil strata toward the frost front. The movement of both liquid water and water vapor occurs in response to these thermally-induced cryosuction gradients in an effort to maintain equilibrium, and the vertical displacement of the soil that occurs as this incoming water freezes is referred to as secondary heave (*28*). Depending on the availability of water, secondary heaving can result in significant vertical displacements and heaving pressures in frost-susceptible soils subjected to sustained freezing temperatures (*29*). A soil does not need to be saturated for either primary or secondary heaving to occur, although individual pore spaces do need to be filled with water for heaving to take place (*11*, *30*).

The two main components of cryosuction are osmotic suction and matric suction (*31*). Osmotic suction is the force potential that comes from the presence of solutes in the pore water (*32*). When ice forms in nature, the ice is devoid of any contaminants that may have been previously present in the water. For this reason, adding salt to water will decrease the temperature at which the water freezes. This decrease in temperature is attributed to the extra energy needed to "freeze out," or exclude, salt ions as the water molecules are incorporated into a crystalline lattice structure characteristic of ice (*14*). As the salt ions accumulate in super-cooled pore water surrounding ice nucleations, the salt concentration increases well above the concentration that existed before freezing. Due to ensuing differences in osmotic suction caused by salt concentration gradients, water then flows from zones of low ion concentrations to zones of high ion concentrations (*33*). Thus, during the winter months when deicing salts are regularly

distributed onto roadways, and as ions existing in the water are "frozen out," an increase in solute concentration will potentially cause water with a lower ion concentration to rise into the frost front, where it will solidify into ice when the temperature falls below the freezing point.

Matric suction is the force potential that comes from the presence of air-water menisci in the soil. Because matric suction is a function of the surface tension in the contractile skin comprising the air-water meniscus, matric suction is inherently linked to osmotic suction because of the increase in surface tension that greater salt concentrations provide (*34*). The intensity of matric suction is also affected by the contact angle at which the water wets the surface of the soil particles and the radius of the air-water meniscus, which is largely determined by the sizes of the soil particles. Higher surface tension, lower contact angles, and smaller radii give rise to greater suction at the air-water interface (*33*). Because coarse-grained materials like gravels contain large particles, the radii of air-water menisci are also comparatively large, and the magnitude of matric suction is therefore low; these materials are usually not frost-susceptible. While clayey soils consist of very small particles that do exhibit significant matric suction, as evidenced by considerable capillary rise potential, they are not sufficiently permeable to water to sustain a growing ice lens and are also not usually frost-susceptible. Silts, however, because they are permeable enough to allow water transport while possessing the required particle-size distribution to create suction potential, are considered highly susceptible to frost heave.

Heaving of frost-susceptible soils can continue as long as water is available, freezing conditions persist, and heaving pressures exceed overburden pressures (*4, 11*). The progression of the frost front into the soil, however, is largely determined by the rate of heat removal from the soil system and the rate at which heat is supplied through the freezing of water at the frost front (*4, 31*). When the latent heat of fusion, or the energy released as water changes from liquid

to solid states, counterbalances the heat removed from the soil, the progression of the frost front stalls, and an ice lens forms at that location (*31*). Once the amount of heat loss exceeds the latent heat of fusion, which can be caused by the onset of colder temperatures or the depletion of the water supply, the frost front continues to advance downward until thermal equilibrium is once again reached. This process repeated through time results in a succession of ice lenses segregated by frozen soil (*4*). Figure 2.1 illustrates the process by which ice lenses form, and Figure 2.2 depicts ice lenses that formed in a frost-susceptible silt during laboratory testing.

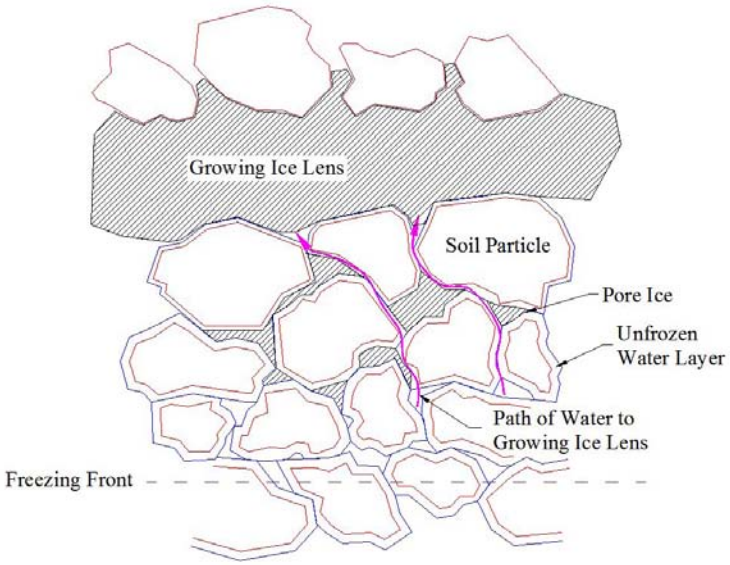

Figure 2.1: Schematic of a growing ice lens (*35*).

Figure 2.2: Ice lenses in a Montana silt (*35*).

2.3 Frost Heave Damage

In the context of pavement performance, frost heave causes damage in two ways. First, the vertical ground displacement during the winter months leads to pavement roughness and cracking, and, second, thawing during spring can lead to substantial reductions in the bearing capacity of affected pavement structures (*18*). The vertical displacement of the ground surface caused by the ingress and freezing of subsurface water within the underlying soil strata causes differential stresses in affected structures. Due to the fact that spatial variability in freezing temperatures, available water, and soil frost-susceptibility is common along many highways, uniform heaving cannot usually be expected. The differential heaving that occurs instead causes surface irregularities and general surface roughness in the form of bumps, waves, and distinctive cracking as shown in Figure 2.3. Severe cases of differential heave will usually cause significantly reduced traffic speeds and may cause damage to automobiles or loss of control of the vehicle (*36*).

Figure 2.3: Pavement damage due to frost heave (*37*).

As the air temperature begins to rise during the spring, the ground begins to thaw from the surface down. However, because drainage of meltwater from upper soil strata is often prevented by the presence of still-frozen underlying soil layers, the soil can become super-saturated and experience marked reductions in bearing capacity (*14*). In this condition, roadway foundation soils do not adequately support the pavement surface layers, which can then experience excessive strain and attendant damage under heavy trafficking (*38*). Furthermore, the susceptibility of pavement structures to damage can increase with repeated cycles of freezing and thawing, depending on the type of soil and the amount of frost heave that occurs (*39*). To minimize such damage, many agencies impose spring load restrictions on affected roads (*40*).

The negative effects of frost action on roads and streets are well documented by maintenance engineers working in cold regions. For example, The Road Information Program (TRIP) estimates that more than $2 billion is required to rebuild the thousands of miles of pavement that are destroyed each winter in the United States. This expenditure does not account

for the cost of filling potholes and resurfacing pavements with minor damage, nor does it account for the cost of automobile repairs resulting from rough pavements or the increased cost of transporting goods because of detours necessary to avoid damaged roads (*36*). Understanding the mechanisms of frost heave and minimizing frost damage to roadways is therefore critical in maintaining a safe and efficient roadway system.

2.4 Summary

Frost heave is a phenomenon that has been studied for over 80 years. When water changes from a liquid to a solid state, it increases in volume by 9 percent. This expansion is known as primary heave. As pore water turns into ice, the soil becomes increasingly devoid of liquid water. This desiccation creates suction forces that cause available water to attempt to move up through the soil strata toward the frost front. The movement of both liquid water and water vapor occurs in response to these thermally-induced cryosuction gradients in an effort to maintain equilibrium, and the vertical displacement of the soil that occurs as this incoming water freezes is referred to as secondary heave. The two main components of cryosuction are osmotic suction and matric suction. Osmotic suction is the force potential that comes from the presence of solutes in the pore water. Matric suction is the force potential that comes from the presence of air-water menisci in the soil. Heaving of frost-susceptible soils can continue as long as water is available, freezing conditions persist, and heaving pressures exceed overburden pressures.

In the context of pavement performance, frost heave causes damage in two ways. First, the vertical ground displacement during the winter months leads to pavement roughness and cracking, and, second, thawing during spring can lead to substantial reductions in the bearing capacity of affected pavement structures. TRIP estimates that more than $2 billion is required to

rebuild the thousands of miles of pavement that are destroyed each winter in the United States. Therefore, understanding the mechanisms of frost heave and minimizing frost damage to roadways is critical in maintaining a safe and efficient roadway system.

3 PROCEDURES

3.1 Overview

In this research, a full-factorial laboratory experiment involving one type of aggregate base material, three thermal gradients, and three fines contents was performed. As described in the following sections, the procedures included material preparation, material characterization, frost heave testing, hydraulic conductivity testing, statistical analysis, and numerical modeling.

3.2 Material Preparation

The aggregate base material and supplementary fines, sent to BYU from Fairbanks, were first distributed into pans and placed into large ovens for drying at 110°C to constant weight. Once dried, the bulk material was separated over the following 10 sieves, as well as the pan: 19 mm, 12.5 mm, 9.5 mm, 4.75 mm, 2.36 mm, 1.18 mm, 600 μm, 300 μm, 150 μm, and 75 μm. Approximately 6 kg of material at a time was sieved for 10 minutes on a large tray shaker to ensure a consistent separation of the bulk material into different size fractions, which were then placed in separate buckets. The materials were then ready to be weighed out in measured proportions as required to match the master gradations provided by UAF research personnel.

3.3 Material Characterization

UAF research personnel classified the bulk material using both the AASHTO and Unified Soil Classification System (USCS) methods. They also determined the optimum moisture

content (OMC) and maximum dry density (MDD) for the material in accordance with American Society for Testing and Materials (ASTM) D1557 (Standard Test Methods for Laboratory Compaction Characteristics of Soil Using Modified Effort (56,000 ft-lbf/ft3 (2,700 kN-m/m3))) and performed soil suction testing to determine the soil-water characteristic curves (SWCCs) following ASTM D2325 (Standard Test Method for Capillary-Moisture Relationships for Coarse- and Medium-Textured Soils by Porous-Plate Apparatus). BYU personnel then determined the apparent specific gravity of the material following ASTM C127 (Specific Gravity and Absorption of Coarse Aggregate) and ASTM C128 (Specific Gravity and Absorption of Fine Aggregate). BYU personnel also evaluated the salinity of the material by measuring the electrical conductivity of a soil solution prepared by adding 5 g of the supplementary fines to 100 g of deionized water. A dual platinum-plate contacting-type electrode was used for this purpose, and three replicate samples were tested.

3.4 Frost Heave Testing

Frost heave testing included mold preparation, specimen preparation, chamber preparation, test operation, and moisture profile determinations. Eighteen molds were prepared for use in this research. Mold preparation involved drilling seven 3.2-mm-diameter holes into the base of each mold to allow water ingress into the sample. In each case, one hole was drilled through the center of the bottom of the mold, while six other holes were drilled around the center hole half way between the center and the edge of the mold as shown in Figure 3.1. Each mold measured 152.4 mm in diameter and 304.8 mm in height. Longitudinal slots 25.4 mm in length were also cut into nine of the 18 molds beginning at distances of 50.8, 76.2, 101.6, 127.0, 152.4, 177.8, and 203.2 mm from the top of the mold. These slots accommodated thermocouples that

were inserted into the samples immediately before the samples were placed into the water bath. In order to ensure that the openings did not overlap one another, the slots at 50.8, 101.6, 152.4, and 203.2 mm were placed in a vertical line on one side of the mold, while the slots at 76.2, 127.0, and 177.8 mm were placed in a vertical line on the opposite side of the mold. After the necessary holes were cut in the molds, the inside of each mold was cleaned and sanded smooth to ensure that no barbs or plastic shavings would interfere with the tests. Appropriate labels were written on each mold in order to identify the specific fines content and thermal gradient associated with each sample. Each of the 18 molds was oiled on the inside just prior to the time of compaction to prevent the soil sample from adfreezing to the mold in the frost heave chamber, which could have impeded the heaving action. A piece of filter paper was placed at the bottom of each mold. The purpose of the filter paper was to minimize seepage of the soil and water through the holes in the bottom of the mold. Finally, each mold was weighed before compaction.

Figure 3.1: Sample molds for frost heave testing.

Specimen preparation consisted of weighing out the material for each sample according to the gradation specified by UAF research personnel. Linear interpolation was necessary to determine weigh-outs for sieve sizes that were not specified but over which the material was separated by BYU personnel to achieve greater precision in replicating sample gradations. The specific sieve sizes used for greater accuracy were 12.5 mm, 1.18 mm, 600 μm, and 150 μm. The samples were calculated to weigh approximately 9.5 kg by dry weight. This value was multiplied by the OMC of 5.3 percent to obtain the weight of water, 0.504 kg. After each set of weigh-outs was completed, the water was added, and the samples were thoroughly mixed, covered, and allowed to equilibrate for at least 24 hours.

The Proctor compaction procedure described in ASTM D1557 was used to compact the samples into the molds. However, because the specimens were twice the size of a typical specimen, twice as many lifts were required; fifty-six blows of a 4.54-kg hammer dropped from a height of 457.2 mm were applied to each of 10 lifts. The top of each lift was scarified before placement of the next lift to facilitate mechanical interlock between lifts. Once the compaction was complete, a finishing tool was used to level the surface of each sample. The 3.86-kg slide hammer on the finishing tool was dropped three times from a height of 457.2 mm, with the tool being rotated one quarter turn between each blow in order to ensure a level surface. The initial height and weight of each sample were then measured and recorded, and the samples were covered and placed inside the frost heave chamber.

Chamber preparation involved lowering the testing room temperature to 1°C and then equilibrating all of the necessary frost heave test equipment and samples for 24 hours prior to the start of each individual test. The components of the frost heave apparatus placed in the chamber included a water bath container, heat tape used to automatically regulate the water bath

temperature, a table used to insulate the water bath, collars placed around sample bases at the height of the table, thermocouples inserted into the sides of selected samples, lateral sample insulation applied to ensure uniaxial heat transfer, 4.54-kg overburden weights to simulate the presence of a pavement surface layer, an overhead frame for holding linear variable differential transformers (LVDTs) employed in the test to automatically measure frost heave, and the data logger used to automatically record thermocouple and LVDT readings. Each frost heave test included six actual samples and three dummy samples so that all nine available test positions were filled. The six actual samples included two replicates of each of the three fines contents investigated in this research, one of which was instrumented with thermocouples as shown in Figure 3.2. In addition to the thermocouples inserted in these samples, three thermocouples were also placed in the bath water, and two were placed in the air within the chamber. These thermocouples were used to monitor the temperatures of the samples, bath water, and air during each test. Although the water bath was filled to the desired depth of 50.8 mm prior to the equilibration period, the samples were not placed into the bath until the end of the equilibration period. Figure 3.3 displays a sample fully prepared for frost-heave testing. The individual samples were then placed into the water bath inside the chamber in specific locations according to a systematic rotation schedule prepared for this research to minimize any effects of location in the water bath on test results. One LVDT was situated above each sample to record actual heave as depicted in Figure 3.4. In order to achieve the three target thermal gradients of 0.15, 0.30, and 0.45ºC/cm, the water bath and air temperatures were individually controlled. The heat tape in the bath water was programmed to keep the bath water at an average temperature of 1°C for all tests. The bath water temperature needed to remain above freezing so that each sample had a continuous liquid water supply. A computer monitored the temperature of the bath; if the bath

Figure 3.2: Sample instrumented with thermocouples.

Figure 3.3: Sample with insulation and overburden weight.

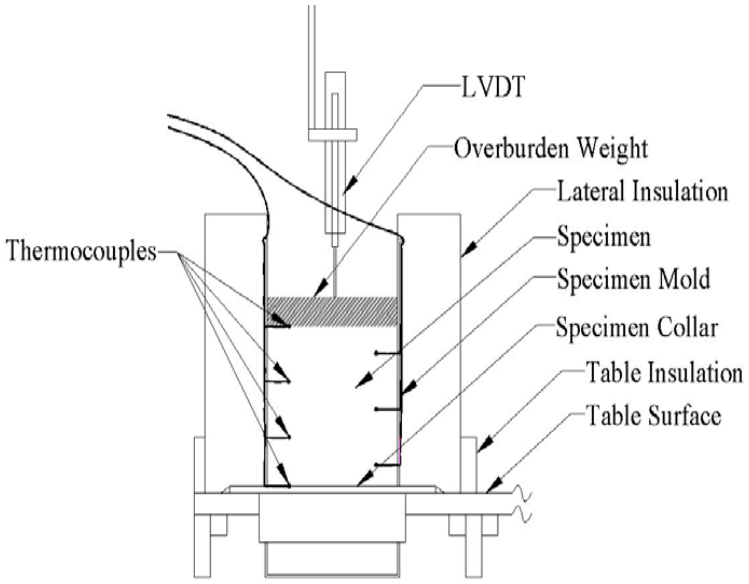

Figure 3.4: Schematic of typical frost heave test configuration (*35*).

water cooled to 0.5°C, the heat tape would turn on and heat the bath water to 1.5°C, at which time the heat tape would turn off. The different thermal gradients were then established by setting the air temperature in the frost heave chamber to -2.43, -5.86° or -9.29°C as required. The sample arrangement for each test is displayed in Figure 3.5.

Test operation included initializing each test and then monitoring the data. Due to the occurrence of equipment difficulties during the frost heave tests involving thermal gradients of 0.15 and 0.45°C/cm, many of the samples partially thawed and subsided while the problems were diagnosed and addressed. After the equipment was repaired and the freezing conditions re-established, the samples were monitored until they had returned to the same height they had achieved just before the equipment failure. The time required for the samples to recover in these cases, 5 days for the batch tested at 0.15°C/cm and 2 days for the batch tested at 0.45°C/cm, was added to the individual test duration. This solution ensured that all samples experienced 20 days of continuous frost heaving. The frost heave test involving the thermal gradient of 0.30°C/cm was completed without any such complications.

8% Fines	Dummy	8% Fines	
6% Fines	Dummy	10% Fines	0.15°C/cm
6% Fines	Dummy	10% Fines	
Front of Chamber			
6% Fines	Dummy	6% Fines	
10% Fines	Dummy	8% Fines	0.30°C/cm
10% Fines	Dummy	8% Fines	
Front of Chamber			
6% Fines	Dummy	8% Fines	
6% Fines	Dummy	8% Fines	0.45°C/cm
10% Fines	Dummy	10% Fines	
Front of Chamber			

Figure 3.5: Sample positions for frost heave testing.

Moisture profiles were determined for individual samples at the conclusion of each frost heave test. The samples were removed from the frost heave chamber, and the final height and weight of each specimen were measured. The samples were then rapidly frozen in a large chest

freezer to preserve the moisture profiles established during testing. Each sample was removed, in turn, from the freezer, weighed, removed from its mold, photographed, and then broken into five lifts of approximately the same mass. These lifts were placed into individual pans and reweighed. Once the weights had been recorded, each pan was placed into an oven set at 110°C until constant weight was achieved. The moisture content was then computed for each lift. The photographs of the samples are provided in the appendix.

3.5 Hydraulic Conductivity Testing

For hydraulic conductivity testing, one sample of aggregate was prepared at each of the three fines contents evaluated in this research. Each sample was weighed out exactly the same way as the frost heave samples and compacted using the modified Proctor protocol. However, to facilitate placement in the permeameter apparatus, these samples were prepared in polyvinyl chloride (PVC) pipe molds that measured 152.4 mm in diameter and 254.0 mm in height. In order to prevent preferential water flow between the sample and the inside of the mold, a 3-mm-thick layer of latex caulking was applied on the inside of the mold as shown in Figure 3.6. The caulking was allowed to cure for 24 hours before a sample was compacted in the mold. Partial aggregate embedment in the caulking during compaction minimized the occurrence of artificially high hydraulic conductivity values during testing.

Due to the delicate nature of the caulking, compactions were performed with a manually operated modified Proctor hammer as shown in Figure 3.7 to ensure the seal was not damaged during the procedure. The compacted samples were then placed in an oven at 60°C for at least 12 hours to allow them to partially dry before they were placed in the permeameter. Drying increased the stiffness of the samples and provided greater stability during subsequent handling.

Figure 3.6: Sample mold for hydraulic conductivity testing.

Figure 3.7: Preparation of sample for hydraulic conductivity testing.

A piece of filter paper was placed between the sample and a screen inside the permeameter to prevent the fines from washing through the apparatus. Once a sample was secured in the permeameter as illustrated in Figure 3.8, approximately 1 m of head was applied for a period of 24 hours, which was determined to be a sufficient amount of time to saturate the samples. A ball valve at the output was closed during this period of time so that the applied water would be contained within the apparatus. After the soaking period was complete, the ball valve was opened, and the water in the pipe above the sample was pressurized to a constant 69 kPa for the samples with 6 and 8 percent fines and 138 kPa for the samples with 10 percent fines. Before each test was initialized, the apparatus was allowed to run for approximately 10 minutes in order to allow the water to reach a steady-state flow rate. The time intervals required to collect cumulative aliquots of 50, 100, 150, 200, 250 and 300 cm^3 of water in a graduated cylinder placed at the permeameter output were carefully measured so that flow rates could be calculated. The time measurements associated with the different volumes were averaged to compute the

Figure 3.8: Typical hydraulic conductivity test configuration.

hydraulic conductivity of a sample. At the end of each test, the sample was removed from the permeameter and broken apart to verify that the entire sample was saturated. Hydraulic conductivity values were computed using Equation 3.1:

$$k = \frac{Q \cdot L}{A \cdot h \cdot t} \tag{3.1}$$

where k = hydraulic conductivity, cm/hr

Q = volume of water passing through the sample, cm^3

L = length of the sample, cm

A = cross sectional area of the sample, cm^2

h = head of water above the sample surface, cm

t = time, hr

3.6 Statistical Analysis

The statistical analyses performed in this research were associated strictly with the frost heave testing and were designed to investigate relationships between the independent, or predictor, variables of thermal gradient and fines content and the various dependent, or response, variables measured in the tests. A stepwise regression analysis was performed to identify significant independent variables for each of nine separate dependent variables, including frost heave, heave-uptake ratio, steady-state frost heave rate, gravimetric water ingress, and gravimetric water content in each of the five individual lifts tested following frost heave testing. In a stepwise regression process, the utility of potential independent variables is assessed using a *p*-value, or level of significance, computed for each independent variable. The independent predictor variables found to be the most influential on the dependent variable are used in the

formation of the regression model. The independent variables used in these analyses were chosen based upon the objectives of the research with respect to studying the effects of thermal gradient and fines content on frost heave behavior; therefore, the independent variables used were thermal gradient, fines content, thermal gradient squared, fines content squared, and the product of thermal gradient and fines content. Independent variables having *p*-values less than 0.15 were allowed to be included in the regression models. However, only those with *p*-values less than or equal to 0.05 were considered statistically significant in predicting the dependent variables. Once a given regression model is formed, an R^2 value, or coefficient of determination, can be computed for the model. The R^2 value reflects the percentage of variation in the dependent variable that is explained by variation in the independent variables included in the regression model, where an R^2 value of 1.0 represents a perfect model (*41*).

3.7 Numerical Modeling

The computer program ICE-1 was utilized in this research for numerical modeling of the frost heave tests. ICE-1 is designed to analyze the coupled flow of water, heat, and solutes in unsaturated, partially frozen soils, including heave effects. The model simultaneously solves equations representing the suction-water content relationship, hydraulic conductivity function, state of energy of the liquid phase, approximate time integral of Darcy's law, approximate time integral of the Fourier heat diffusion equation, and the mass balance of solutes. The simulated one-dimensional soil column is divided into 1-cm-thick elements for analysis. The program requires the following inputs: sample length, slope of the transformed SWCC, initial osmotic pressure, cooling rate, hydraulic conductivity, overburden weight, porosity, volumetric water content, initial soil temperature, simulation increment, simulation time, air-entry water potential,

and lower boundary soil temperature. All of these parameters were specifically measured for the tested samples except for the initial osmotic pressure, which was instead estimated from the results of the electrical conductivity testing. In ICE-1, two conditions may be specified at the lower boundary: either a zero-water-flow boundary or a flux boundary. In this research, a flux boundary condition was chosen to simulate the actual laboratory frost heave test configuration, which allowed the movement of water from the water bath into the samples. The program computes and displays temperature, liquid water content, total water content, salt content, heaving pressure, and overburden pressure for each given depth element. It also computes latent heat and total heave.

3.8 Summary

In this research, a full-factorial laboratory experiment involving one type of aggregate base material, three thermal gradients, and three fines contents was performed. Each of the three frost heave tests incorporated six actual samples and three dummy samples. The six actual samples included two replicates of each of the three fines contents investigated in this research, one of which was instrumented with thermocouples. In addition, one LVDT was situated above each sample to record actual heave. The specified thermal gradients of 0.15, 0.30, and 0.45ºC/cm were then established by setting the air temperature in the frost heave chamber to -2.43, -5.86, or -9.29°C, as required. The heat tape in the bath water was programmed to keep the bath water at an average temperature of 1°C for all tests. Test operation included initializing each test and then monitoring the data. Moisture profiles were determined for individual samples at the conclusion of each frost heave test. Each sample was removed, in turn, from the freezer and broken into five lifts of approximately the same mass. A stepwise regression

analysis was performed to identify significant independent variables for each of nine separate dependent variables, including frost heave, heave-uptake ratio, steady-state frost heave rate, gravimetric water ingress, and gravimetric water content in each of the five individual lifts tested following frost heave testing. Soil suction, specific gravity, salinity, and hydraulic conductivity testing were also performed on samples prepared at each of the three fines contents to support numerical modeling of the results of the frost heave tests using the computer program ICE-1. ICE-1 is designed to analyze the coupled flow of water, heat, and solutes in unsaturated, partially frozen soils, including heave effects.

4 RESULTS

4.1 Overview

The following sections present the results of the testing and analyses performed in this research, including material preparation, material characterization, frost heave testing, hydraulic conductivity testing, statistical analysis, and numerical modeling. These results should only be applied to materials and conditions similar to those investigated in this research.

4.2 Material Preparation

The grain-size distribution of the bulk Alaska base material is shown in Figure 4.1. The supplementary fines provided by UAF personnel were used to meet the gradation requirement for particles finer than the 0.075-mm sieve.

4.3 Material Characterization

The classification of the Fairbanks material was performed by UAF research assistants. According to the AASHTO system, the material was classified as an A-1-a soil for all three fines contents of 6, 8, and 10 percent. According to the USCS, the material was classified as GW-GM for the gradation containing 6 and 8 percent fines and as GP-GM for the gradation containing 10 percent fines. The OMC for all three gradations was determined to be 5.3 percent by weight of

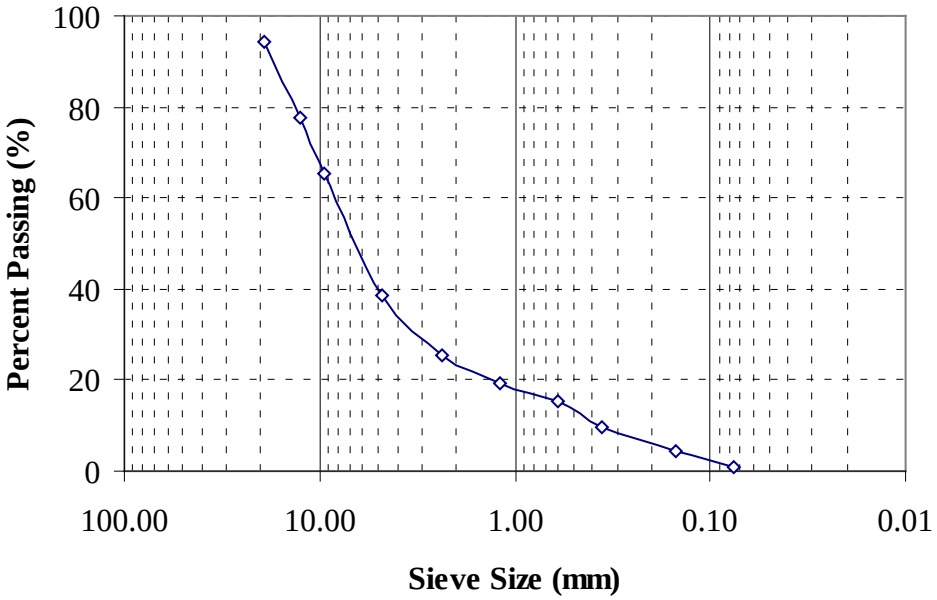

Figure 4.1: Particle-size distribution for bulk material.

dry material, and the MDD was determined to be 2340, 2370, and 2372 kg/m^3 for the gradations having fines contents of 6, 8, and 10 percent, respectively. The SWCCs are shown in Figure 4.2.

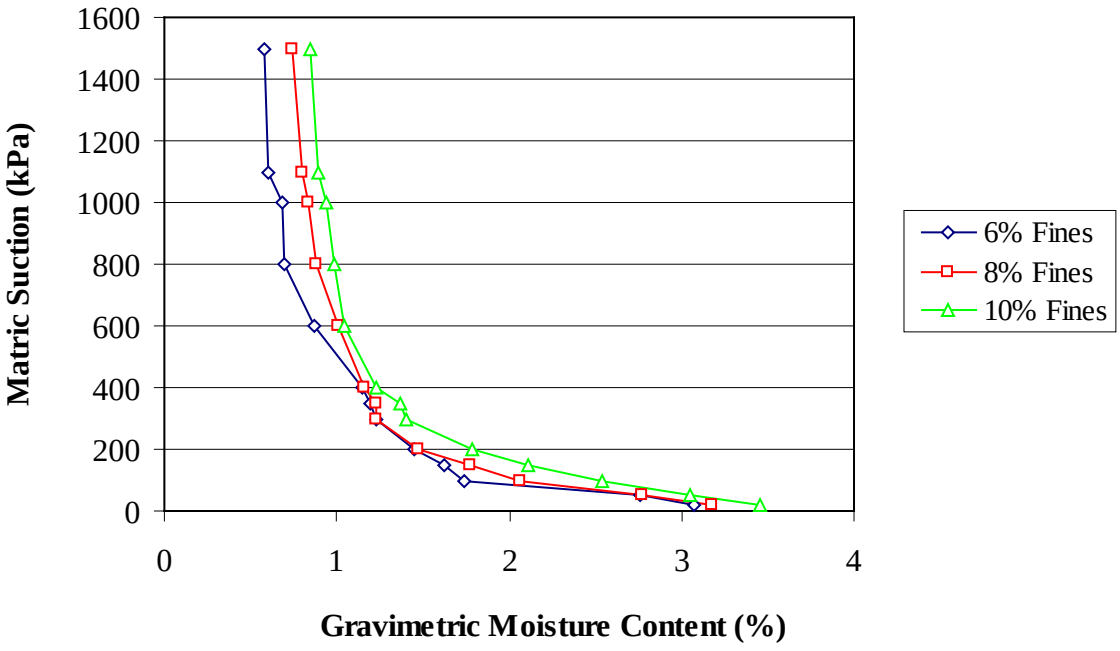

Figure 4.2: Soil-water characteristic curves.

Figure 4.3 shows the transformed SWCCs that were developed from those in Figure 4.2 to facilitate calculation of the slopes and air-entry water potentials needed for numerical modeling of the observed frost heave behavior according to the general model given in Equation 4.1 (*42*). Equations 4.2, 4.3, and 4.4 were developed from the transformed SWCCs for the fines contents of 6, 8, and 10 percent, respectively, using linear regression.

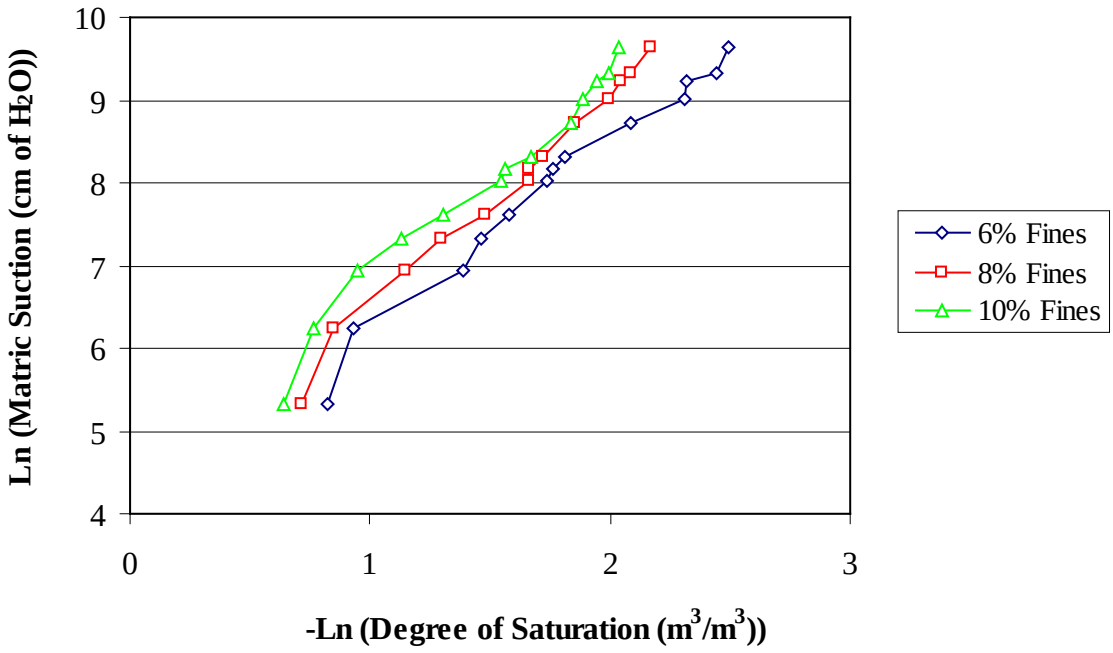

Figure 4.3: Transformed soil-water characteristic curves.

$$\ln\psi = b\left(-\ln\left(\frac{\theta}{n}\right)\right) + \ln\psi_e \qquad (4.1)$$

where ψ = matric suction, cm of water

ψ_e = air-entry water potential, cm of water

θ = volumetric water content, $\frac{m^3}{m^3}$

n = porosity, $\frac{m^3}{m^3}$

b = slope of soil-water characteristic curve

$$y = 2.3188 \cdot x - 3.8628 \quad (R^2 = 0.9736) \tag{4.2}$$

$$y = 2.7007 \cdot x - 3.6933 \quad (R^2 = 0.9879) \tag{4.3}$$

$$y = 2.6159 \cdot x - 4.1118 \quad (R^2 = 0.9725) \tag{4.4}$$

The values of apparent specific gravity for the coarse and fine materials were determined to be 2.71 and 2.69, respectively; these values appropriately averaged produce a harmonic mean of 2.70 for the blended material used to create samples in this research. The results of the three individual conductivity tests performed on the supplementary fines were 106, 108, and 101 µS/cm.

4.4 Frost Heave Testing

The final weigh-outs for each gradation are displayed in Table 4.1. Table 4.2 presents the data collected during the frost heave tests. Hyphens in the table represent data that could not be measured due to negative water ingress. Temperature profiles corresponding to the steady-state frost heave rate for each test were measured using the thermocouples with which selected samples were instrumented. Based on these readings, the actual thermal gradients within the samples were determined to be 0.06, 0.11, and 0.25°C/cm for the target thermal gradients of

Table 4.1: Sample Weigh-Outs

Sieve Size	Weigh-Outs (kg)		
	6% Fines	8% Fines	10% Fines
19 mm	0	0	0
12.5 mm	1.744	1.708	1.671
9.5 mm	0.872	0.854	0.836
4.75 mm	2.440	2.383	2.331
2.36 mm	1.454	1.425	1.394
1.18 mm	0.907	1.032	1.009
600 μm	0.672	0.509	0.498
300 μm	0.461	0.450	0.440
150 μm	0.419	0.413	0.404
75 μm	0.206	0.203	0.199
pan	0.586	0.781	0.976

0.15, 0.30, and 0.45°C/cm, respectively, that were imposed as boundary conditions on the samples in this research. The target bath water and air temperatures for each test were also verified by the collected thermocouple data. Graphs depicting the actual readings of these thermocouples are given in the appendix. These graphs indicate that the water bath temperature never dropped below 0°C and implies that the lower portion of each sample, which was immersed in the water bath, also remained unfrozen throughout the tests. This observation applies even to those tests that were performed at thermal gradients of 0.30 and 0.45°C/cm, in which the portions of the samples above the water line froze after only 5 and 2 days, respectively. In these cases, the rate at which heat was removed from the samples exceeded the rate at which heat from the water bath could rise through the samples, causing the frost front to descend rather quickly toward the bottoms of the samples. Then, due to insufficient matric

Table 4.2: Frost Heave Data

Thermal Gradient (°C/cm)	Fines Content (%)	Sample	Dry Density (kg/m^3)	Initial Total Volume (m^3)	Porosity (%)	Gravimetric Water Content				Volumetric Water Content				Final Total Volume (m^3)	Initial Height (mm)	Final Height (mm)	Frost Heave (mm)	Heave Volume (m^3)	Heave-Uptake Ratio (m^3/m^3)	Steady-State Frost Heave Rate (mm/hr)
						Initial (%)	Final (%)	Ingress (%)	Ingress (kg)	Initial (%)	Final (%)	Ingress (%)	Ingress (m^3)							
0.15	6	1	2256	0.0043	16.5	5.3	7.4	2.1	0.200	12.1	16.1	4.0	0.0002	0.0045	235.0	244.2	9.2	0.0002	0.839	0.0273
		2	2276	0.0043	15.8	5.3	7.3	2.0	0.185	12.2	15.9	3.7	0.0002	0.0044	233.2	242.9	9.7	0.0002	0.952	0.0265
		Ave	2266	0.0043	16.1	5.3	7.3	2.0	0.193	12.1	16.0	3.9	0.0002	0.0044	234.1	243.5	9.4	0.0002	0.896	0.0269
	8	1	2306	0.0042	14.7	5.3	7.5	2.2	0.207	12.3	16.2	3.9	0.0002	0.0045	230.3	245.0	14.7	0.0003	1.293	0.0251
		2	2296	0.0042	15.0	5.3	7.6	2.3	0.216	12.3	16.4	4.1	0.0002	0.0045	231.2	244.9	13.6	0.0002	1.153	0.0224
		Ave	2301	0.0042	14.8	5.3	7.5	2.2	0.211	12.3	16.3	4.0	0.0002	0.0045	230.8	244.9	14.2	0.0003	1.223	0.0237
	10	1	2293	0.0042	15.1	5.3	7.2	1.9	0.177	12.2	15.5	3.2	0.0002	0.0045	231.8	245.8	14.0	0.0003	1.447	0.0248
		2	2276	0.0043	15.8	5.3	7.3	2.0	0.185	12.1	15.8	3.7	0.0002	0.0044	233.8	243.4	9.7	0.0002	0.953	0.0271
		Ave	2284	0.0042	15.4	5.3	7.2	1.9	0.181	12.2	15.7	3.5	0.0002	0.0045	232.8	244.6	11.8	0.0002	1.200	0.0259
0.30	6	1	2248	0.0043	16.8	5.3	5.9	0.6	0.051	12.0	13.0	1.0	0.0001	0.0044	236.8	240.5	3.7	0.0001	1.325	0.0027
		2	2261	0.0043	16.3	5.3	5.7	0.4	0.038	12.1	12.8	0.7	0.0000	0.0043	235.1	238.4	3.3	0.0001	1.569	0.0010
		Ave	2254	0.0043	16.6	5.3	5.8	0.5	0.044	12.0	12.9	0.8	0.0000	0.0044	235.9	239.4	3.5	0.0001	1.447	0.0018
	8	1	2299	0.0042	14.9	5.3	5.6	0.3	0.028	12.3	12.6	0.4	0.0000	0.0043	230.8	236.6	5.9	0.0001	3.774	0.0055
		2	2294	0.0042	15.1	5.3	5.7	0.4	0.035	12.2	12.9	0.7	0.0000	0.0043	232.1	234.8	2.6	0.0000	1.379	0.0044
		Ave	2297	0.0042	15.0	5.3	5.7	0.4	0.032	12.3	12.8	0.5	0.0000	0.0043	231.4	235.7	4.3	0.0001	2.576	0.0049
	10	1	2280	0.0043	15.6	5.3	7.8	2.5	0.235	12.1	17.3	5.1	0.0002	0.0044	233.7	239.0	5.3	0.0001	0.412	0.0076
		2	2305	0.0042	14.7	5.3	6.0	0.7	0.064	12.3	13.6	1.3	0.0001	0.0043	231.2	234.9	3.7	0.0001	1.057	0.0108
		Ave	2293	0.0042	15.1	5.3	6.9	1.6	0.150	12.2	15.4	3.2	0.0001	0.0043	232.4	237.0	4.5	0.0001	0.734	0.0092
0.45	6	1	2302	0.0042	14.8	5.3	5.3	0.0	-0.017	12.3	11.7	-0.6	0.0000	0.0043	230.3	234.0	3.7	0.0001	-	0.0008
		2	2293	0.0042	15.1	5.3	5.4	0.1	0.000	12.2	12.1	-0.1	0.0000	0.0043	232.1	234.3	2.2	0.0000	-	0.0014
		Ave	2297	0.0042	15.0	5.3	5.3	0.1	0.000	12.3	11.9	-0.4	0.0000	0.0043	231.2	234.1	3.0	0.0001	-	0.0011
	8	1	2304	0.0042	14.7	5.3	5.3	0.0	-0.008	12.3	11.9	-0.4	0.0000	0.0043	230.7	233.9	3.1	0.0001	-	0.0015
		2	2293	0.0042	15.1	5.3	5.4	0.1	0.008	12.2	12.2	0.0	0.0000	0.0043	232.4	235.5	3.1	0.0001	7.060	0.0014
		Ave	2299	0.0042	14.9	5.3	5.4	0.1	0.008	12.3	12.1	0.0	0.0000	0.0043	231.6	234.7	3.1	0.0001	7.060	0.0014
	10	1	2309	0.0042	14.5	5.3	5.4	0.1	0.009	12.3	12.3	0.0	0.0000	0.0043	230.6	233.9	3.2	0.0001	6.825	0.0014
		2	2310	0.0042	14.5	5.3	5.4	0.1	0.006	12.3	12.4	0.0	0.0000	0.0042	230.1	232.3	2.1	0.0000	6.126	0.0014
		Ave	2310	0.0042	14.5	5.3	5.4	0.1	0.007	12.3	12.3	0.0	0.0000	0.0043	230.4	233.1	2.7	0.0000	6.475	0.0014

suction and/or the apparently low hydraulic conductivity of the samples at the frost front, conditions were not suitable for the formation of ice lenses. Increases in the sample heights were therefore limited mainly to those occurring from primary heave.

The pertinent results from each frost heave test were the average total frost heave, heave-uptake ratio, steady-state frost heave rate, and gravimetric water ingress. The total amount of frost heave exhibited by each sample was calculated by subtracting the initial height from the final height of each sample. The heave-uptake ratio was computed as the ratio of heave volume that each sample experienced to the water volume imbibed by the sample from the water bath during testing. A heave-uptake ratio of 1.09 indicates that all of the water that entered the sample contributed to frost heave, as water expands 9 percent by volume when it freezes. A heave-uptake ratio of less than 1.09 indicates that the porosity of the soil was sufficient to allow the water to expand inside the soil matrix without causing frost heave. A ratio higher than 1.09 indicates that the sample experienced upward redistributions of existing water during the freezing process that gave rise to measurable heave above and beyond that associated with the ingress of additional water from the water bath. Heave-uptake ratios are only meaningful in this research for samples that imbibed water beyond the OMC. The steady-state frost heave rate was determined for each sample from plots of heave versus time. Although the time required to achieve steady-state behavior varied among the samples, a constant rate of frost heave was eventually achieved by all samples tested. The gravimetric water ingress was calculated by subtracting the initial gravimetric water content, which was equal to the OMC, from the final gravimetric water content, which was determined from the weights of each sample measured at the end of the corresponding test and after the sample was oven-dried.

The moisture gradients for the tests performed at thermal gradients of 0.15, 0.30, and 0.45°C/cm are displayed in Figures 4.4, 4.5, and 4.6, respectively, in which the depth shown for each data point is the distance from the surface of the specimen to the center of a given lift.

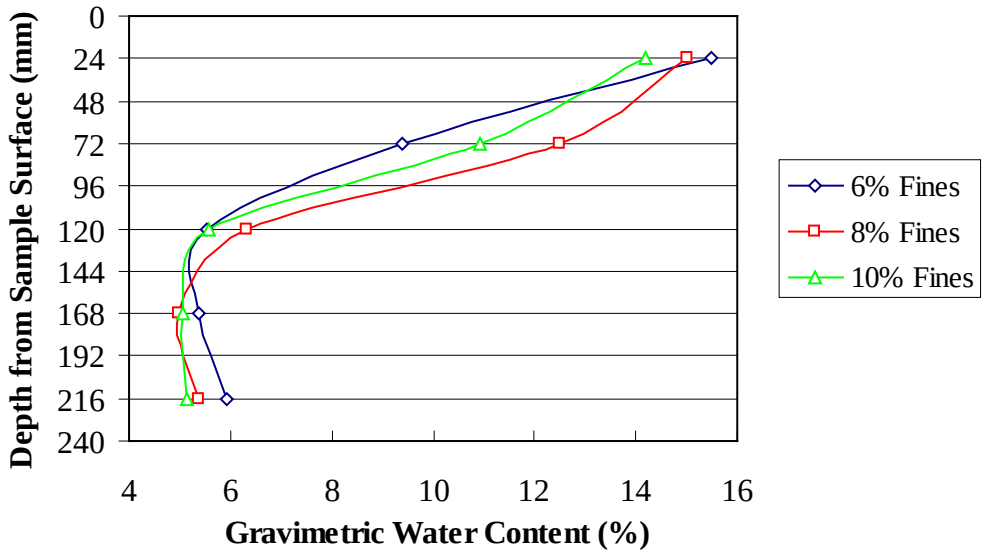

Figure 4.4: Moisture gradients for samples tested at thermal gradient of 0.15°C/ cm.

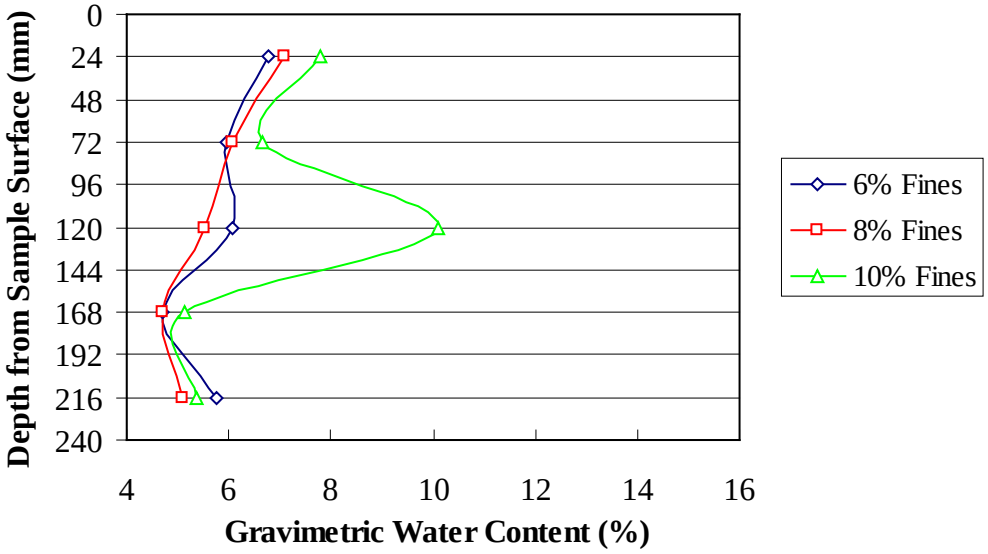

Figure 4.5: Moisture gradients for samples tested at thermal gradient of 0.30°C/cm.

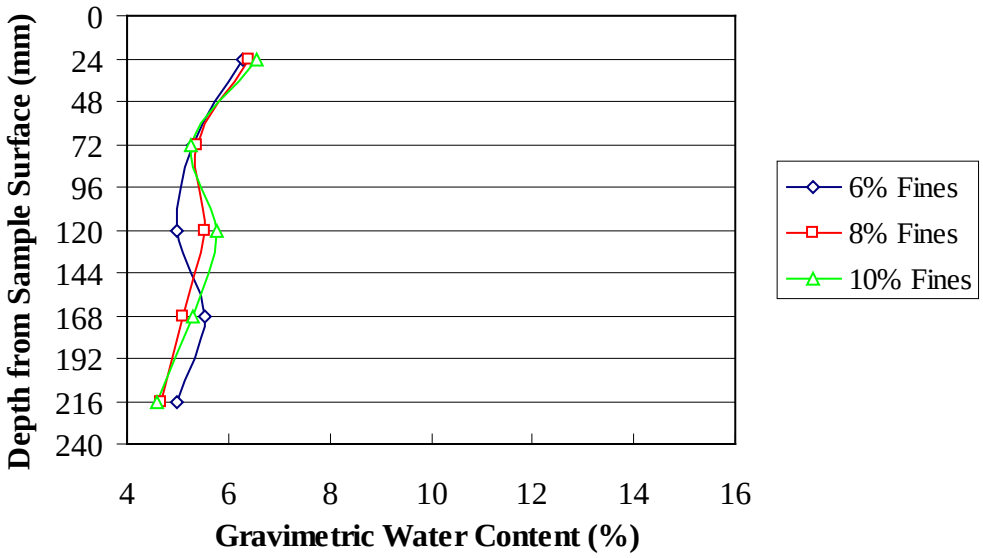

Figure 4.6: Moisture gradients for samples tested at thermal gradient of 0.45°C/cm.

Depths with water contents below the OMC of 5.3 percent experienced desiccation during the test as water was redistributed from those locations upwards towards the freezing front. Statistical analyses of these data are presented in Section 4.6.

4.5 Hydraulic Conductivity Testing

The measurements obtained during hydraulic conductivity testing are shown in Table 4.3. For computation of hydraulic conductivity in each case, values of 22.86 cm, 15.24 cm, and 182.41 cm^2 were used for the sample length, diameter, and cross-sectional area, respectively. The total head used to calculate hydraulic conductivity included the water head and air pressure inside the PVC pipe that was situated over the samples. Average saturated hydraulic conductivity values for samples with 6, 8, and 10 percent fines were computed to be 0.0649, 0.0469, and 0.0230 cm/hr, respectively.

Table 4.3: Hydraulic Conductivity Data

Fines Content (%)	Water Head (cm)	Water Volume Collected (cm^3)	Collection Time (hr)	Saturated Hydraulic Conductivity (cm/hr)
6	802.4	50	0.13	0.0605
		100	0.25	0.0661
		150	0.37	0.0625
		200	0.50	0.0598
		250	0.60	0.0770
		300	0.72	0.0661
8	802.4	50	0.15	0.0530
		100	0.32	0.0453
		150	0.53	0.0380
		200	0.67	0.0530
		250	0.83	0.0485
		300	1.00	0.0469
10	1505.8	50	0.17	0.0250
		100	0.34	0.0246
		150	0.52	0.0230
		200	0.68	0.0250
		250	0.89	0.0204
		300	1.08	0.0212

4.6 Statistical Analysis

Table 4.4 shows the *p*-values computed in the stepwise regression for each factor. As described in Section 3.6, only factors having *p*-values less than or equal to 0.15 were included; the hyphens in the table indicate that the *p*-values in those cases exceeded 0.15. Factors with *p*-values less than or equal to 0.05 were considered to be statistically significant in this research. These data indicate that thermal gradient is a significant predictor of frost heave, heave-uptake

ratio, steady-state heave rate, gravimetric water ingress, and gravimetric water content in the first and second lifts and that the square of thermal gradient is a significant predictor of five of these six dependent variables; as the thermal gradient increased, the samples experienced decreasing amounts of water ingress and frost heave. However, the data show that neither fines content nor the square of fines content is a significant predictor of any of the dependent variables, even though the latter was included in models for predicting the steady-state frost heave rate and the gravimetric water content of the third lift; that is, although previous research has shown that higher fines contents are generally associated with greater susceptibility to frost heave, this effect is not manifest in the comparatively small increases in fines contents evaluated in this research. The interaction between thermal gradient and fines content is a significant predictor of only the gravimetric water content in the fifth lift. The stepwise regression analysis resulted in the following Equations 4.5 through 4.12:

Table 4.4: Results of Statistical Analyses on Frost Heave Data

Dependent Variables	*P*-Values for Independent Variables				
	Thermal Gradient	Fines Content	Thermal Gradient * Fines Content	Thermal Gradient Squared	Fines Content Squared
Frost Heave	<0.001	-	-	0.001	-
Heave-Uptake Ratio	0.001	-	-	<0.001	-
Steady-State Frost Heave Rate	<0.001	-	-	<0.001	0.08
Gravimetric Water Ingress	<0.001	-	-	-	-
Gravimetric Water Content in Lift 1	<0.001	-	-	<0.001	-
Gravimetric Water Content in Lift 2	0.001	-	-	0.011	-
Gravimetric Water Content in Lift 3	-	-	-	-	0.14
Gravimetric Water Content in Lift 4	-	-	-	-	-
Gravimetric Water Content in Lift 5	-	-	<0.001	-	-

$$H = 146 \cdot G^2 - 117.2 \cdot G + 26.11 \ (R^2 = 0.870) \quad (4.5)$$

$$Ro = 104.5 \cdot G^2 - 44 \cdot G + 5.3285 \ (R^2 = 0.923) \quad (4.6)$$

$$Rt = 0.36 \cdot G^2 + 0.00004 \cdot F^2 - 0.2964 \cdot G + 0.0595 \ (R^2 = 0.970) \quad (4.7)$$

$$W = -6.66 \cdot G + 2.979 \ (R^2 = 0.761) \quad (4.8)$$

$$L1 = 153 \cdot G^2 - 120.2 \cdot G + 29.5 \ (R^2 = 0.954) \quad (4.9)$$

$$L2 = 85 \cdot G^2 - 69.5 \cdot G + 19.47 \ (R^2 = 0.811) \quad (4.10)$$

$$L3 = 0.026 \cdot F^2 + 4.430 \ (R^2 = 0.131) \quad (4.11)$$

$$L5 = -0.312 \cdot G \cdot F + 5.965 \ (R^2 = 0.592) \quad (4.12)$$

where H = frost heave, mm

G = thermal gradient, °C/cm

Ro = heave uptake ratio, m^3/m^3

Rt = steady-state frost heave rate, mm/hr

F = gravimetric fines content, %

W = gravimetric water ingress, %

L1 = gravimetric water content in the first lift, %

L2 = gravimetric water content in the second lift, %

L3 = gravimetric water content in the third lift, %

L5 = gravimetric water content in the fifth lift, %

An equation for the fourth lift is not given because none of the independent variables were chosen as predictor values for the gravimetric water content of this lift.

Figures 4.7 to 4.12 show the main effect of thermal gradient on frost heave, heave-uptake ratio, steady-state heave rate, gravimetric water ingress, and gravimetric water content in the first and second lifts, and Figure 4.13 shows the interaction between thermal gradient and fines content for gravimetric water content in the fifth lift. Except for the heave-uptake ratio, all of the dependent variables exhibit decreasing values with increasing thermal gradient. The only main effect that was not statistically significant but for which an equation was developed is plotted in the appendix.

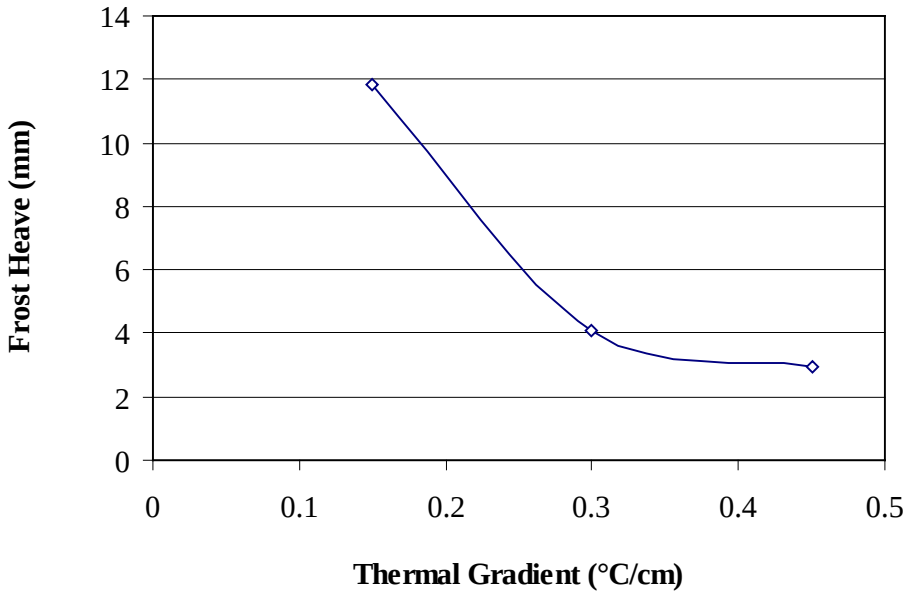

Figure 4.7: Main effect of thermal gradient on frost heave.

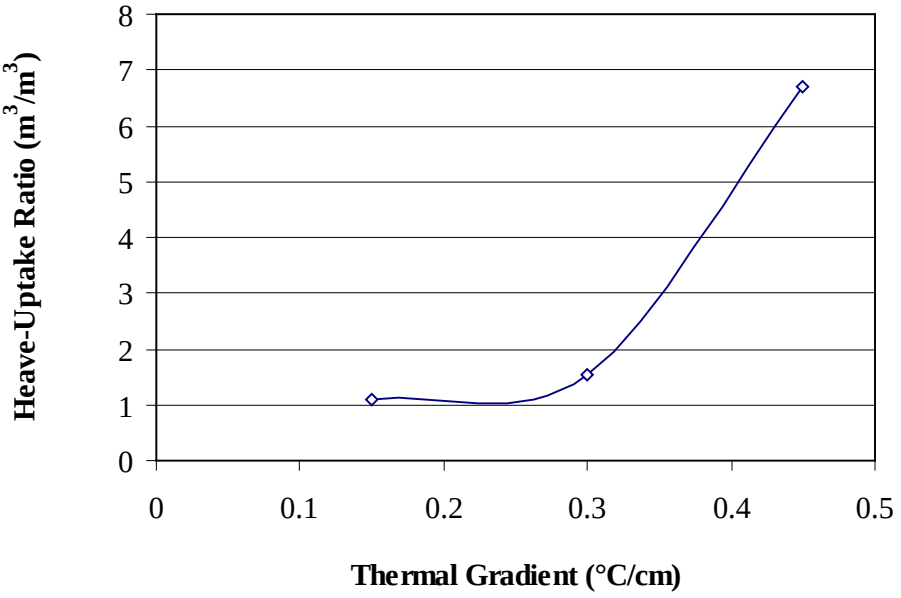

Figure 4.8: Main effect of thermal gradient on heave-uptake ratio.

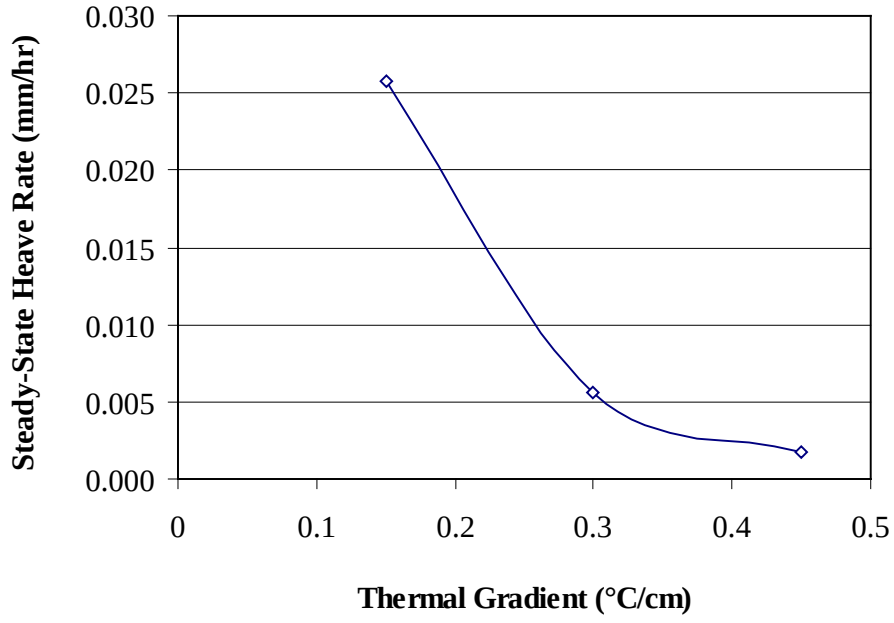

Figure 4.9: Main effect of thermal gradient on steady-state heave rate.

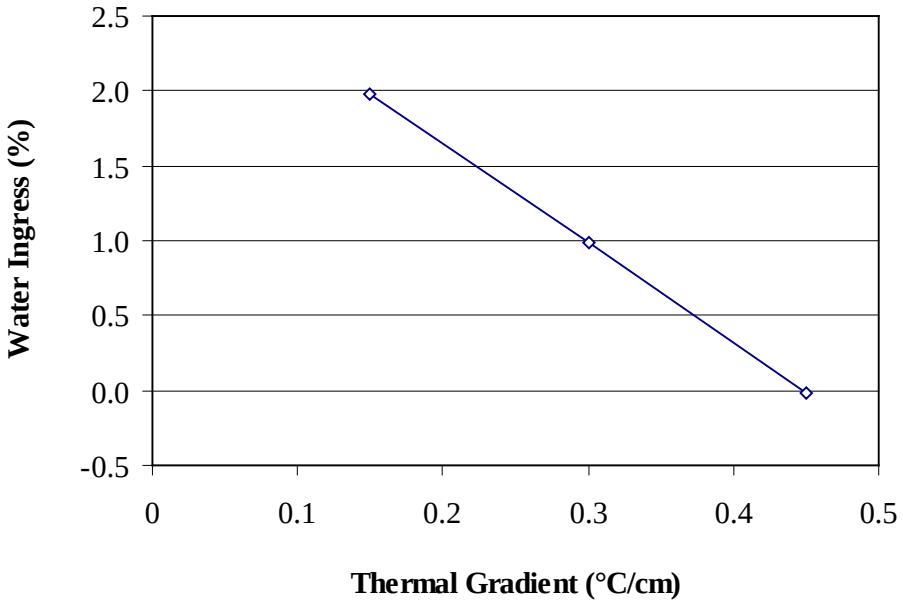

Figure 4.10: Main effect of thermal gradient on water ingress.

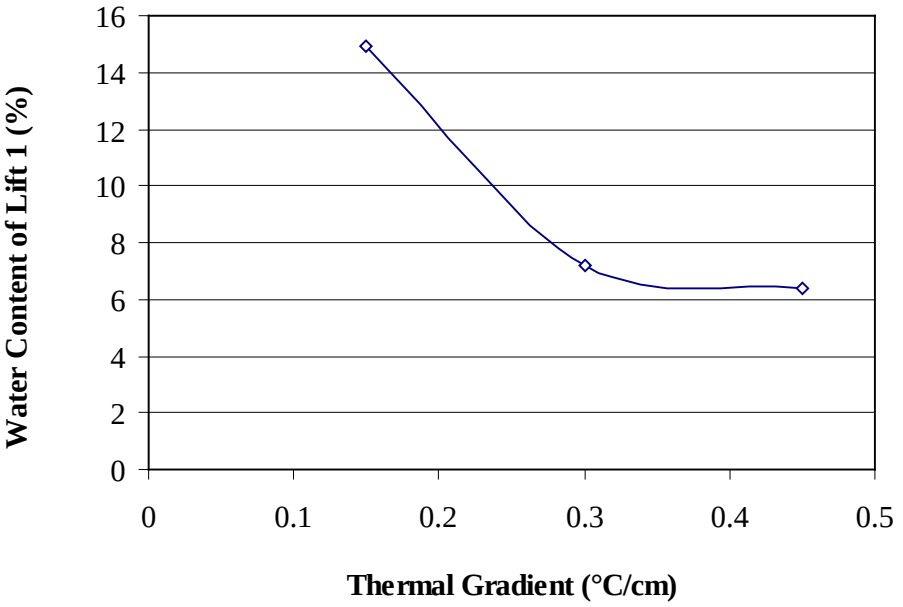

Figure 4.11: Main effect of thermal gradient on water content of lift 1.

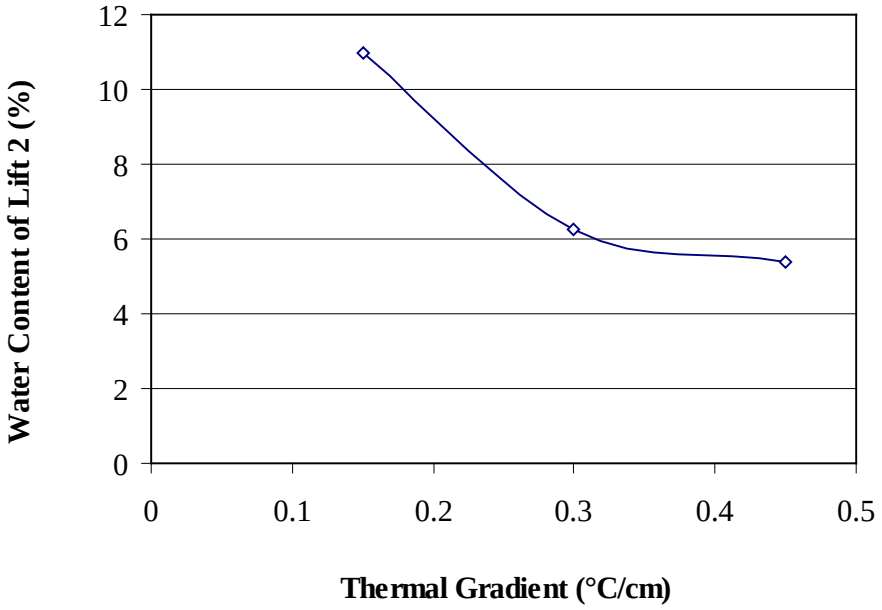

Figure 4.12: Main effect of thermal gradient on water content of lift 2.

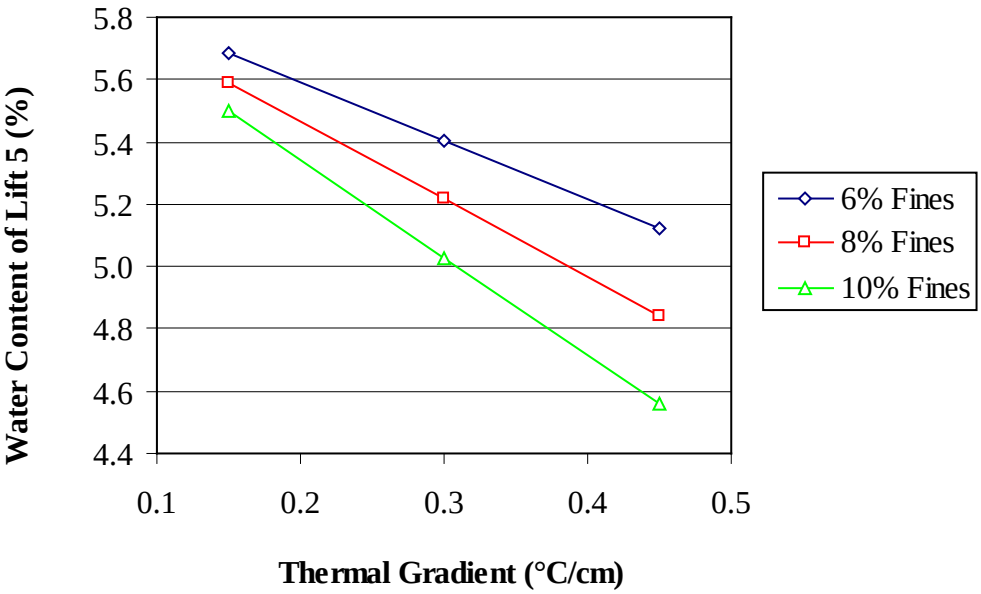

Figure 4.13: Interaction between thermal gradient and fines content for water content of lift 5.

4.7 Numerical Modeling

The input parameters used in the ICE-1 modeling are shown in Tables 4.5 and 4.6, with the values shown in Table 4.6 being held constant for all thermal gradients and fines contents. The values of porosity and initial volumetric water content shown in Table 4.5 are the average values reported in Table 4.2 for a given fines content, and the values of hydraulic conductivity are the average values computed from Table 4.3. The SWCC slopes and air-entry water potentials were obtained from Equations 4.2 to 4.4, and the cooling rates were calculated from temperature measurements obtained using thermocouples situated at the surface of instrumented samples. The soil freezing limit is the same as the air temperature specified for the environmental chamber for a given test. The electrical conductivity test results were analyzed to determine the initial osmotic pressure for use in ICE-1. An estimate of the initial osmotic pressure was determined from the electrical conductivity test results based on the dilution ratio

Table 4.5: Variable Numerical Model Inputs

Thermal Gradient (°C/cm)	Fines Content (%)	Porosity	Volumetric Water Content	Saturated Hydraulic Conductivity (cm/hr)	SWCC Slope	Air-Entry Water Potential (cm of H_2O)	Surface Cooling Rate (°C/hr)	Soil Freezing Limit (°C)
0.15	6	0.159	0.121	0.0649	2.32	47.6	0.009	-2.43
	8	0.149	0.123	0.0469	2.70	40.2	0.009	-2.43
	10	0.150	0.122	0.0230	2.62	61.1	0.009	-2.43
0.30	6	0.159	0.121	0.0649	2.32	47.6	0.025	-5.86
	8	0.149	0.123	0.0469	2.70	40.2	0.025	-5.86
	10	0.150	0.122	0.0230	2.62	61.1	0.025	-5.86
0.45	6	0.159	0.121	0.0649	2.32	47.6	0.04	-9.29
	8	0.149	0.123	0.0469	2.70	40.2	0.04	-9.29
	10	0.150	0.122	0.0230	2.62	61.1	0.04	-9.29

Table 4.6: Constant Numerical Model Inputs

Sample Length (cm)	22.9
Initial Osmotic Pressure (cm of H_20)	1100
Overburden Weight (cm of H_2O)	24.9
Initial Soil Temperature (°C)	1
Time Increment (hr)	0.01
Simulation Time (hr)	480

used in the test, the initial water content of the frost heave samples, an assumption that sodium chloride was the predominant dissolved salt, published data on the electrical conductivity of sodium chloride solutions, and the following Equation 4.13 (*42*):

$$\pi = -\nu \cdot \phi \cdot m \cdot R \cdot T \qquad (4.13)$$

where $\pi =$ osmotic potential, $\frac{\text{J}}{\text{kg}}$

$\nu =$ number of ions per salt molecule

$\phi =$ osmotic coefficient

$m =$ molal solute concentration, $\frac{\text{mol}}{\text{kg}}$

$R =$ gas constant, 8.314 $\frac{\text{J}}{\text{mol K}}$

$T =$ temperature, K

The results of the ICE-1 analyses and a comparison to the results of the frost heave tests are shown in Table 4.7. Differences between the modeled and measured frost heave values range from 0.01 to 0.92 cm, with the larger differences typically associated with the lowest

Table 4.7: Results of Numerical Modeling of Frost Heave Data

Thermal Gradient (°C/cm)	Fines Content (%)	Frost Heave (cm)		
		Measured	Modeled	Difference
0.15	6	0.95	0.32	0.63
	8	1.42	0.72	0.70
	10	1.18	0.35	0.83
0.30	6	0.35	0.94	0.59
	8	0.43	1.29	0.86
	10	0.45	0.53	0.08
0.45	6	0.30	1.22	0.92
	8	0.31	0.32	0.01
	10	0.27	0.64	0.37

thermal gradient and the lowest fines content. The ICE-1 program was therefore more accurate in predicting frost heave for the higher thermal gradients and higher fines contents. Nonetheless, although AKDOT personnel may consider using ICE-1 for predicting frost heave of aggregate base materials, selected laboratory testing to confirm the accuracy of the modeling should probably still be performed.

4.8 Summary

The pertinent results from each frost heave test were the average total frost heave, heave-uptake ratio, steady-state frost heave rate, and gravimetric water ingress. The results of the stepwise regression analysis indicate that thermal gradient is a significant predictor of frost heave, heave-uptake ratio, steady-state heave rate, gravimetric water ingress, and gravimetric water content in the first and second lifts and that the square of thermal gradient is a significant predictor of five of these six dependent variables. As the thermal gradient increased, the samples experienced decreasing amounts of water ingress and frost heave, attributable to the fact that the

increasing rate of heat extraction caused mainly primary heaving to occur. However, the data show that neither fines content nor the square of fines content is a significant predictor of any of the dependent variables, even though the latter was included in models for predicting the steady-state frost heave rate and the gravimetric water content of the third lift. Thus, in summary, although previous research has shown that higher fines contents are generally associated with greater susceptibility to frost heave, this effect is not manifest in the comparatively small increases in fines contents evaluated in this research. The interaction between thermal gradient and fines content is a significant predictor of only the gravimetric water content in the fifth lift.

The results of the ICE-1 analyses when compared to the results of the frost heave tests show differences between the modeled and measured frost heave values that range from 0.01 to 0.92 cm, with the larger differences typically associated with the lowest thermal gradient and the lowest fines content. The ICE-1 program was therefore more accurate in predicting frost heave for the higher thermal gradients and higher fines contents. Nonetheless, although AKDOT personnel may consider using ICE-1 for predicting frost heave of aggregate base materials, selected laboratory testing to confirm the accuracy of the modeling should probably still be performed.

5 CONCLUSION

5.1 Summary

Understanding the mechanics of frost heave is important because it has the potential to cause catastrophic damage to roads, pipelines, bridges, and structures. In order for frost heave to occur, three elements must be present: sustained freezing temperatures, an available water source, and a frost-susceptible material. The susceptibility of a soil to frost heave is commonly determined by the individual grain sizes of the soil particles. To limit frost heave of pavement structures, personnel at AKDOT, in particular, specify a maximum of 6 percent finer than the 0.075-mm sieve for aggregate base materials to be used in construction of Alaska highways. As high-quality aggregate is not readily available in many parts of Alaska, however, AKDOT engineers have become interested in revising the materials specifications to permit the statewide use of lesser-quality aggregates containing more fines. Because Alaska is so geographically distributed, a variety of thermal gradients exist at different locations in the state. While previous research has addressed the effect of fines content on frost heave, the interaction between thermal gradient and fines content has not been specifically investigated. Knowing if the effect of fines depends upon the magnitude of thermal gradient is essential for AKDOT engineers considering applications of new specifications statewide. Therefore, BYU research personnel in partnership with researchers at UAF undertook a research project designed to investigate the effects of thermal gradient and fines content and the interaction between these two factors on the frost heave characteristics of a typical Alaska base material.

The laboratory frost heave testing associated with this research involved one type of aggregate base material, three thermal gradients, and three fines contents. Two replicate specimens were created for each unique combination, yielding a total of 18 test specimens. The material used for this project was classified by the AASHTO classification system as an A-1-a granular soil. This material was sampled from Fairbanks, Alaska, and was supplied by UAF research personnel. Supplementary fines were also supplied from Fairbanks and were added to each of the 18 samples to achieve fines contents, defined as the percentage by mass finer than the 0.075 mm sieve, of 6, 8, and 10 percent. Three thermal gradients, including 0.15, 0.30, and 0.45 ºC/cm, were selected to represent different geographic regions of Alaska. Each of the three frost heave tests incorporated six samples with two replicates of each of the three fines contents investigated in this research, one of which was instrumented with thermocouples. In addition, one LVDT was situated above each sample to record actual heave. The specified thermal gradients of 0.15, 0.30, and 0.45ºC/cm were then established by setting the air temperature in the frost heave chamber to -2.43, -5.86, or -9.29°C, as required. The heat tape in the bath water was programmed to keep the bath water at an average temperature of 1°C for all tests. Test operation included initializing each test and then monitoring the data. Moisture profiles were determined for individual samples at the conclusion of each frost heave test. Each sample was removed, in turn, from the freezer and broken into five lifts of approximately the same mass. A stepwise regression analysis was performed to identify significant independent variables for each of nine separate dependent variables, including frost heave, heave-uptake ratio, steady-state frost heave rate, gravimetric water ingress, and gravimetric water content in each of the five individual lifts tested following frost heave testing. Soil suction, specific gravity, salinity, and hydraulic conductivity testing were also performed on samples prepared at each of the three fines contents

to support numerical modeling of the results of the frost heave tests using the computer program ICE-1. ICE-1 is designed to analyze the coupled flow of water, heat, and solutes in unsaturated, partially frozen soils, including heave effects. The results of this research project are only applicable to the specific soil type, thermal gradients, and fines contents investigated in this research.

5.2 Findings

From this study the pertinent results from each frost heave test were the average total frost heave, heave-uptake ratio, steady-state frost heave rate, and gravimetric water ingress. The results of the stepwise regression analysis indicate that thermal gradient is a significant predictor of frost heave, heave-uptake ratio, steady-state heave rate, gravimetric water ingress, and gravimetric water content in the first and second lifts and that the square of thermal gradient is a significant predictor of five of these six dependent variables. As the thermal gradient increased, the samples experienced decreasing amounts of water ingress and frost heave, attributable to the fact that the increasing rate of heat extraction caused mainly primary heaving to occur. However, the data show that neither fines content nor the square of fines content is a significant predictor of any of the dependent variables, even though the latter was included in models for predicting the steady-state frost heave rate and the gravimetric water content of the third lift. Thus, in summary, although previous research has shown that higher fines contents are generally associated with greater susceptibility to frost heave, this effect is not manifest in the comparatively small increases in fines contents evaluated in this research. The interaction between thermal gradient and fines content is a significant predictor of only the gravimetric water content in the fifth lift.

The results of the ICE-1 analyses when compared to the results of the frost heave tests show differences between the modeled and measured frost heave values that range from 0.01 to 0.92 cm, with the larger differences typically associated with the lowest thermal gradient and the lowest fines content. The ICE-1 program was therefore more accurate in predicting frost heave for the higher thermal gradients and higher fines contents.

5.3 Recommendations

AKDOT personnel should consider revising the materials specifications to permit the use of lesser-quality aggregates containing more fines in areas that exhibit the type of thermal gradients chosen for this study if susceptibility to frost heave is the primary concern. The maximum allowable material finer than the 0.075-mm sieve for aggregate base materials to be used in construction of Alaska highways in these areas can be increased to 10 percent by dry weight of aggregate for materials similar to that evaluated in this research. Consideration of fines contents higher than 10 percent would require further testing, however. AKDOT personnel may also consider using ICE-1 for predicting frost heave of aggregate base materials; however, selected laboratory testing to confirm the accuracy of the modeling should probably still be performed. Additional research on the effect of different fines contents on the resilient modulus or other relevant structural properties of base materials containing elevated fines contents should also be considered, as well as testing of other types of base materials.

REFERENCES

1. Henry, K. S., and R. D. Holtz. Geocomposite Capillary Barriers to Reduce Frost Heave in Soils. *Canadian Geotechnical Journal*, Vol. 38, No. 4, 2001, pp. 678-694.

2. Cary, J. W., R. I. Papendick, and G. S. Campbell. Water and Salt Movement in Unsaturated Frozen Soil: Principles and Field Observation. *Soil Science Society of America Proceedings*, Vol. 43, No. 1, 1979, pp. 3-8.

3. Konrad, J. M., G. Dore, and M. Roy. Field Observations of Instrumented Highway Sections with Different Frost Protections. In *Proceedings of the American Society of Civil Engineers Eighth International Conference on Cold Regions Engineering, Fairbanks, Alaska*. CD-ROM. American Society of Civil Engineers, Reston, VA, August 1996.

4. Penner, E. Ground Freezing and Frost Heaving. *Canadian Building Digest*, CBD-26, National Research Council, Canada, 1962. http://irc.nrc-cnrc.gc.ca/pubs/cbd/cbd026_e.html. Accessed June 26, 2008.

5. Konrad, J. M. The Influence of Heat Extraction Rate in Freezing Soils. *Cold Regions Science and Technology*, Vol. 14, No. 2, 1987, pp. 129-137.

6. Konrad, J. M., and N. R. Morgenstern. Prediction of Frost Heave in the Laboratory during Transient Freezing. *Canadian Geotechnical Journal*, Vol. 19, No. 3, 1982, pp. 250-259.

7. Konrad, J. M. Frost Susceptibility Related to Soil Index Properties. *Canadian Geotechnical Journal*, Vol. 36, No. 3, 1999, pp. 403-417.

8. Penner, E. Influence of Freezing Rate on Frost Heaving. In *Highway Research Record 393*, Highway Research Board, National Research Council, Washington, DC, 1972, pp. 56-64.

9. Doré, G., J. M. Konrad, and M. Roy. Deterioration Model for Pavements in Frost Conditions. In *Transportation Research Record: Journal of the Transportation Research Board*, No. 1655, Transportation Research Board of the National Academies, Washington, D.C., 1999, pp. 110-117.

10. Brown, W. G. Frost Heave in Ice Rinks and Cold Storage Buildings. *Canadian Builders Digest*, No. 61, 1965.

11. Hermansson, A., and W. S. Guthrie. Frost Heave and Water Uptake Rates in Silty Soil Subject to Variable Water Table Height during Freezing. *Cold Regions Science and Technology*, Vol. 43, No. 3, 2005, pp. 128-139.

12. Cary, J. W., and H. F. Mayland. Salt and Water Movement in Unsaturated Frozen Soil. *Soil Science Society of America Proceedings*, Vol. 36, No. 4, 1972, pp. 549-555.

13. Panday, S., and M. Y. Corapcioglu. Solute Rejection in Freezing Soils. *Water Resources Research*, Vol. 27, No. 1, 1991, pp. 99-108.

14. Guthrie, W. S., and H. Zhan. Solute Effects on Long-Duration Frost Heave Behavior of Limestone Aggregates. In *Transportation Research Record: Journal of the Transportation Research Board*, No. 1786, Transportation Research Board, National Research Council, Washington, DC, 2002, pp. 112-119.

15. Saarenketo, T. Electrical Properties of Water in Clay and Silty Soils. *Journal of Applied Geophysics*, Vol. 40, 1998, pp. 73-88.

16. Cary, J. W. A New Method for Calculating Frost Heave Including Solute Effects. *Water Resources Research*, Vol. 23, No. 8, 1987, pp. 1620-1624.

17. Kubo, H., and K. Takeichi. Seasonal Nondestructive Evaluation of Frost-Heave Prevention Layer in Asphalt Pavements. In *Transportation Research Record: Journal of the Transportation Research Board*, No. 1362, Transportation Research Board, National Research Council, Washington, DC, 1992, pp. 90-94.

18. Freitag, D. R., and T. McFadden. *Introduction to Cold Regions Engineering.* ASCE Press, New York, NY, 1997.

19. Tester, R. E., and P. N. Gaskin. Effect of Fines Content on Frost Heave. *Canadian Geotechnical Journal,* Vol. 33, No. 4, 1996, pp. 678-680.

20. Guthrie, W. S., and Å. Hermansson. Frost Heave and Water Uptake Relations in Variably Saturated Aggregate Base Materials. In *Transportation Research Record: Journal of the Transportation Research Board*, No. 1821, Transportation Research Board, National Research Council, Washington, DC, 2003, pp. 13-19.

21. Chamberlain, E. J., P. N. Gaskin, D. Esch, and R. L. Berg. *Survey of Methods for Classifying Frost Susceptibility*. American Society of Civil Engineers Technical Council on Cold Regions Engineering Monograph. ASCE Press, New York, NY, 1984, pp. 105-142.

22. Janoo, V. C., L. A. Barna, and S. A. Orchino. *Frost Susceptibility Testing and Predictions for the Raymark Superfund Site*. Report No. A539433. U.S. Army Cold Regions Research and Engineering Laboratory, Hanover, NH, 1997.

23. Bouyoucos, G. J. Degree of Temperature to Which Soils Can Be Cooled without Freezing. *Journal of Agricultural Research*, Vol. 20, No. 4, 1920, pp. 267-269.

24. Taber, S. Frost Heaving. *Journal of Geology*, Vol. 37, No. 5, 1929, pp. 428-461.

25. Taber, S. The Mechanics of Frost Heaving. *Journal of Geology*, Vol. 38, No. 4, 1930, pp. 303-317.

26. Taber, S. Freezing and Thawing of Soils as Factors in the Destruction of Road Pavements. *Public Roads*, Vol. 11, No. 8, 1930, pp. 113-132.

27. Black, P. B., and M. J. Haradenberg. Historical Perspective in Frost Heave Research: The Early Works of S. Taber and G. Beskow. CRREL Special Report 91-23. U.S. Army Cold Regions Research and Engineering Laboratory, Hanover, NH, 1991, pp. 37–157.

28. Perfect, E., R. D. Miller, and B. Burton. Frost Upheaval of Overwintering Plants: A Quantitative Field Study of the Displacement Process. *Arctic and Alpine Research*, Vol. 20, No. 1, 1988, pp. 70-75.

29. Fowler, A. C. Secondary Frost Heave in Freezing Soils. *SIAM Journal on Applied Mathematics*, Vol. 49, No. 4, 1989, pp. 991-1008.

30. Miller, R. D. Freezing and Heaving of Saturated and Unsaturated Soils. In *Highway Research Record 393*, Highway Research Board, National Research Council, Washington, DC, 1972, pp. 1-11.

31. Fredlund, D. G., J. K. Gan, and H. Rahardjo. Measuring Negative Pore Water Pressures in a Freezing Environment. In *Transportation Research Record*: *Journal of the Transportation Research Board*, No. 1307, Transportation Research Board, National Research Council, Washington, DC, 1991, pp. 291-299.

32. Hanks, R. J., and G. L. Ashcroft. *Applied Soil Physics.* Springer-Verlag, New York, NY, 1980.

33. Guthrie, W. S., Å. Hermansson, and T. Scullion. Determining Aggregate Frost Susceptibility with the Tube Suction Test. In *Cold Regions Engineering: Cold Regions Impacts on Transportation and Infrastructure*. American Society of Civil Engineers, Reston, VA, May 2002, pp. 663-674.

34. Weast, R. C., D. R. Lide, M. J. Astle, and W. H. Beyer, Eds. *CRC Handbook of Chemistry and Physics*. CRC Press, Inc., Boca Raton, FL, 1989.

35. Lay, R. D. *Development of a Frost Heave Test Apparatus*. M.S. thesis. Department of Civil and Environmental Engineering, Brigham Young University, Provo, UT, 2005.

36. Dimillio, A. *A Quarter Century of Geotechnical Research.* Publication FHWA-RD-98-139. FHWA, U.S. Department of Transportation, Washington, DC, 1998.

37. http://www.ringcycles.blogspot.com. Accessed May 22, 2010.

38. Doré, G., J. M. Konrad, and M. Roy. Role of Deicing Salt in Pavement Deterioration by Frost Action. In *Transportation Research Record: Journal of the Transportation Research Board*, No. 1596, Transportation Research Board of the National Academies, Washington, D.C., 1997, pp. 70-75.

39. Vinson, T. S., J. W. Rooney, and W. H. Haas. *Roads and Airfields in Cold Regions: A State of the Practice Report.* American Society of Civil Engineers, Reston, VA, 1996.

40. Spring Load Restrictions. Office of Materials and Road Research, Minnesota Department of Transportation, St. Paul, MN. http://www.mrr.dot.state.mn.us/research/seasonal_load_limits/thawindex/tfs_slr.asp. Accessed May 22, 2010.

41. Ott, R. L., and M. Longnecker. *An Introduction to Statistical Methods and Data Analysis*, Fifth Edition. Duxbury, Pacific Grove, CA, 2001.

42. Guthrie, W. S. *Effects of Deicing Salt on Physical Properties of Aggregate Base Material*. Ph.D. dissertation. Department of Civil Engineering, Texas A&M University, College Station, TX, 2002.

APPENDIX

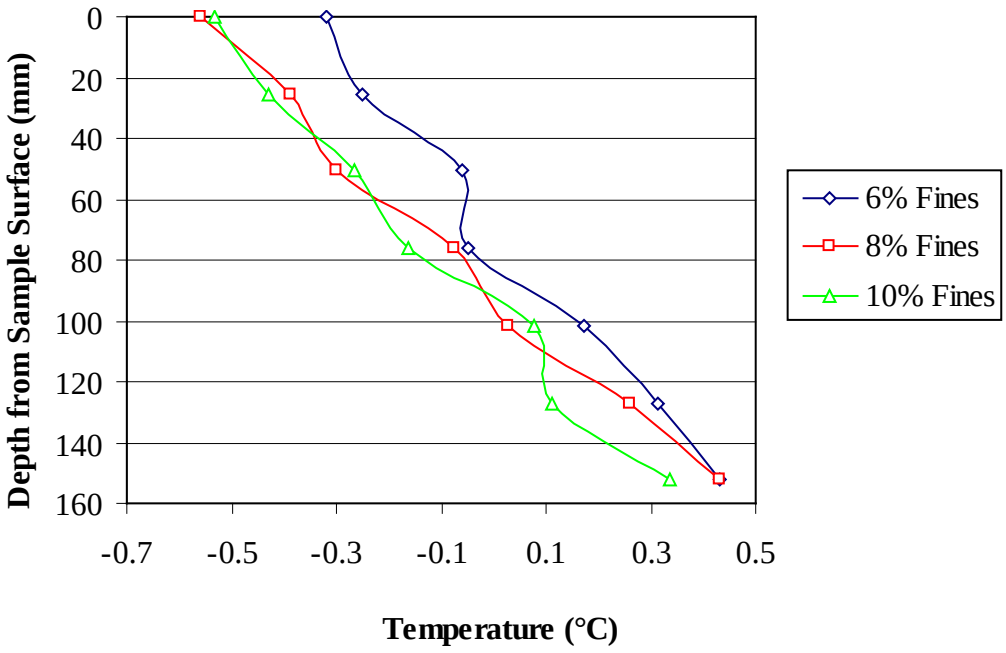

Figure A.1: Steady-state temperature profile for thermal gradient of 0.15°C/cm.

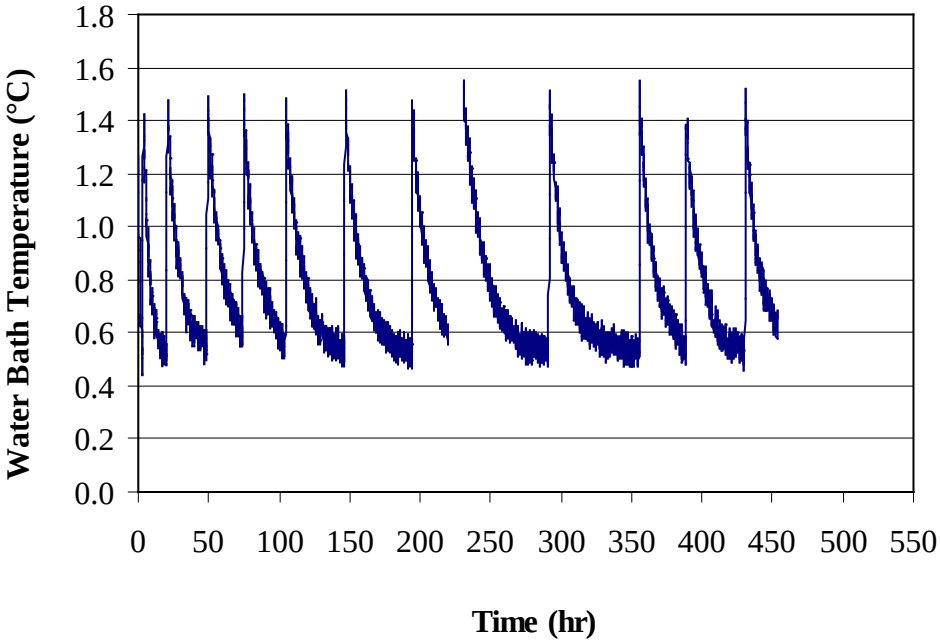

Figure A.2: Water bath temperature for thermal gradient of 0.15°C/cm.

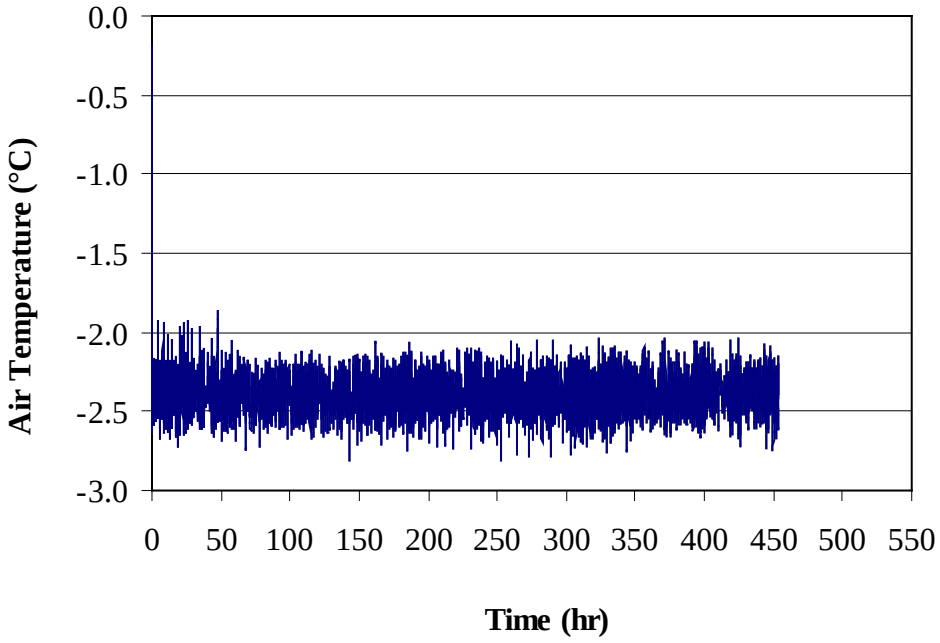

Figure A.3: Air temperature for thermal gradient of 0.15°C/cm.

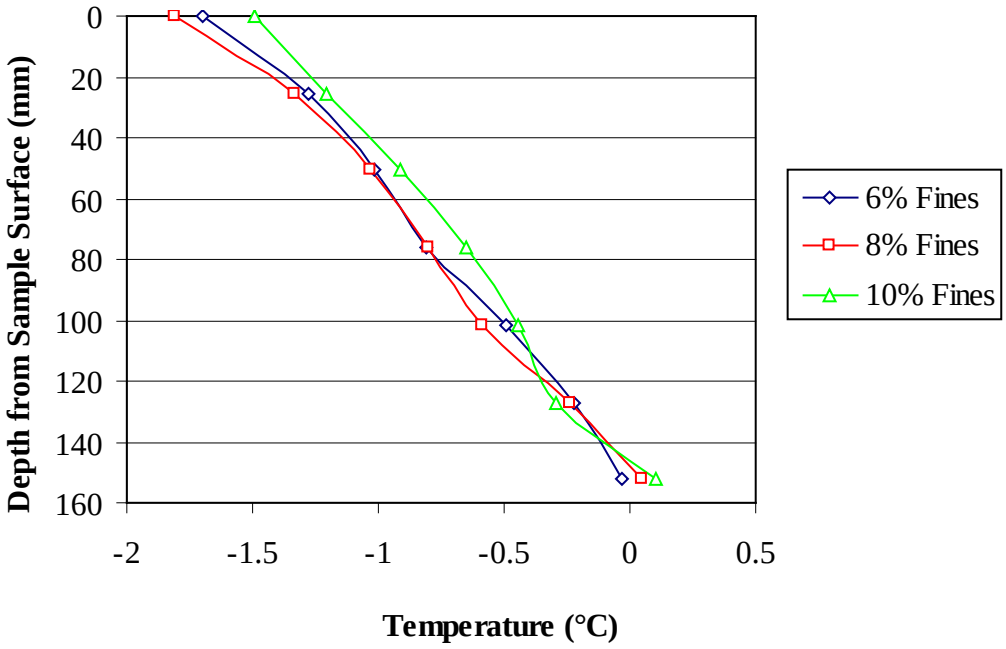

Figure A.4: Steady-state temperature profile for thermal gradient of 0.30°C/cm.

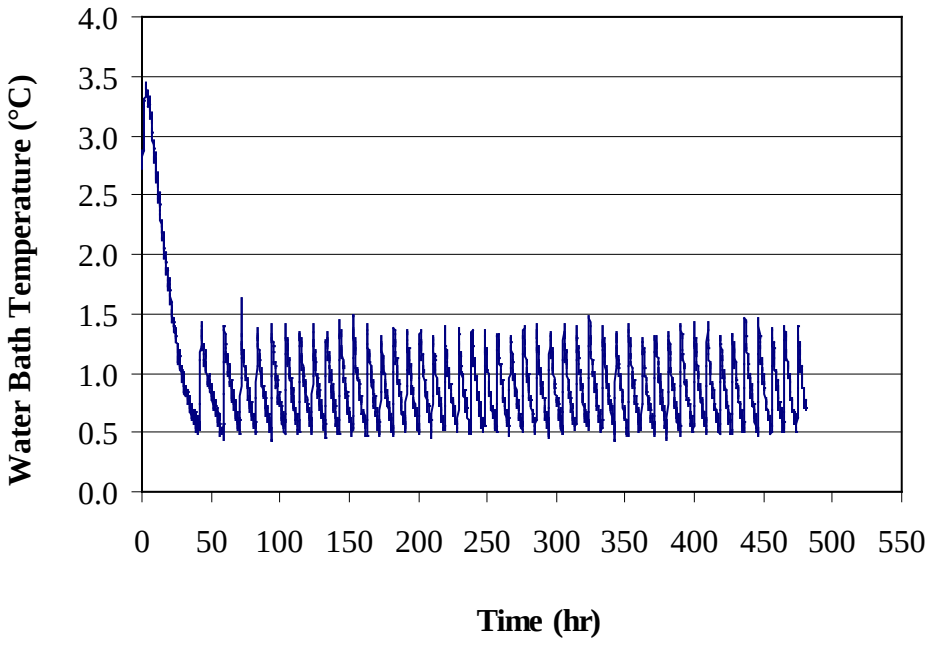

Figure A.5: Water bath temperature for thermal gradient of 0.30°C/cm.

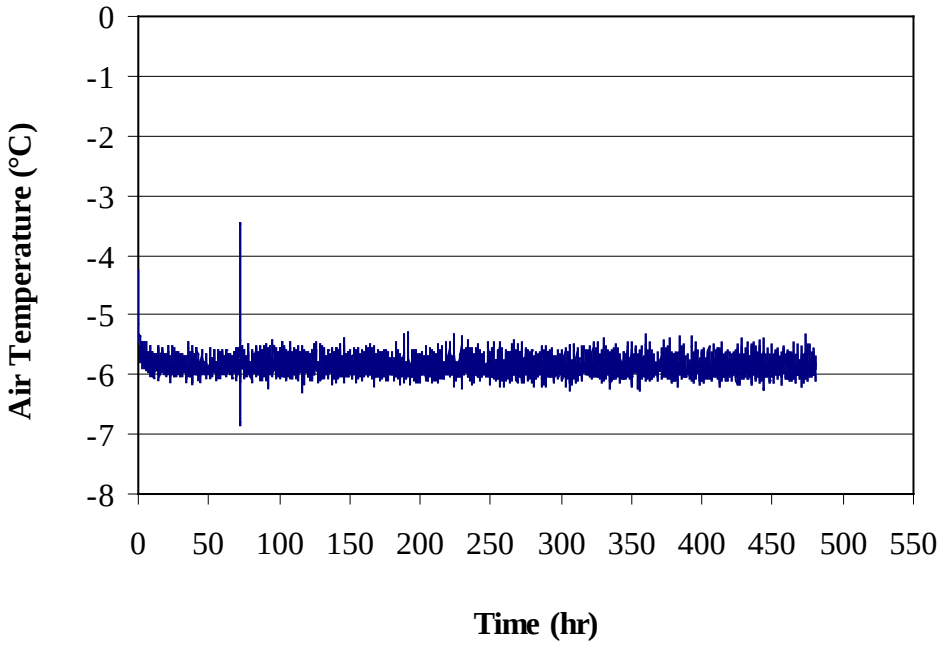

Figure A.6: Air temperature for thermal gradient of 0.30°C/cm.

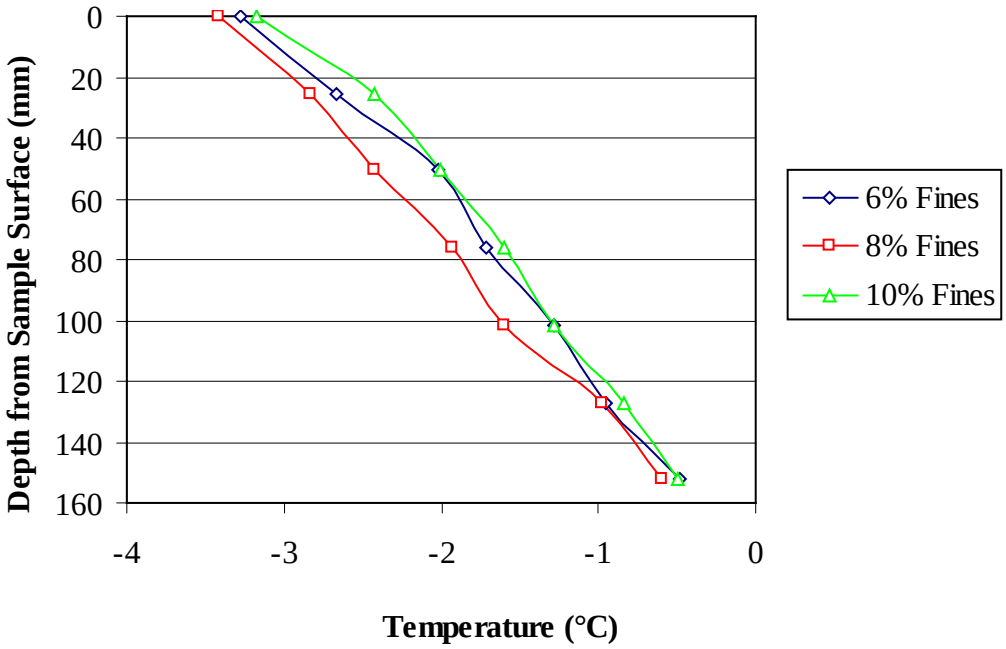

Figure A.7: Steady-state temperature profile for thermal gradient of 0.45°C/cm.

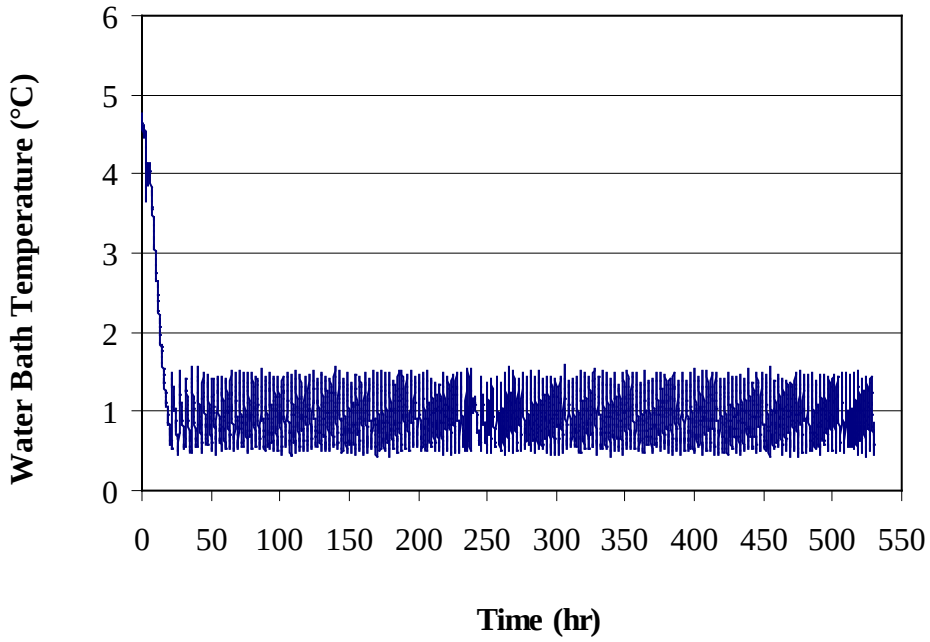

Figure A.8: Water bath temperature for thermal gradient of 0.45°C/cm.

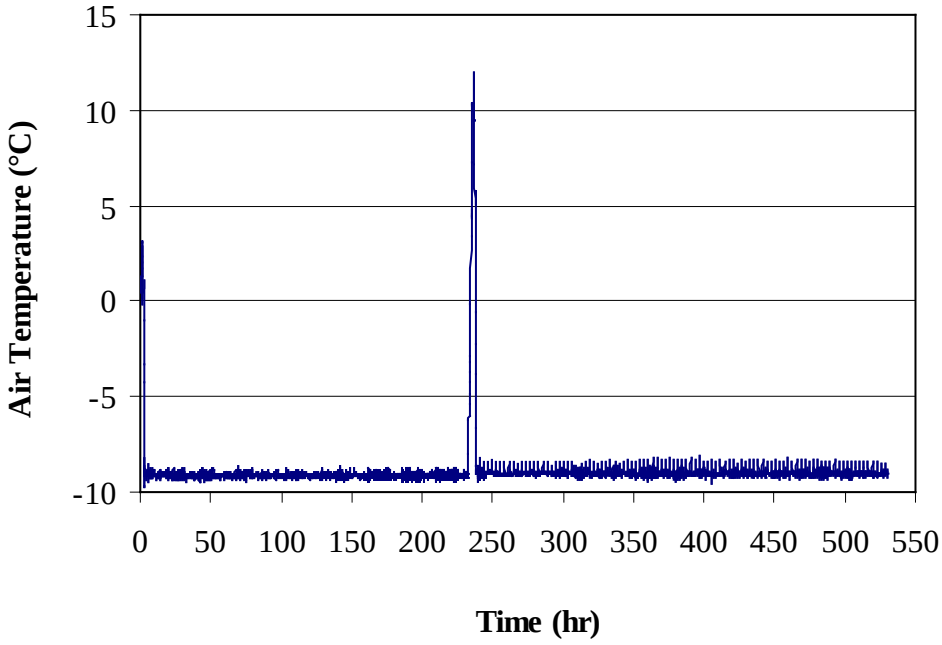

Figure A.9: Air temperature for thermal gradient of 0.45°C/cm.

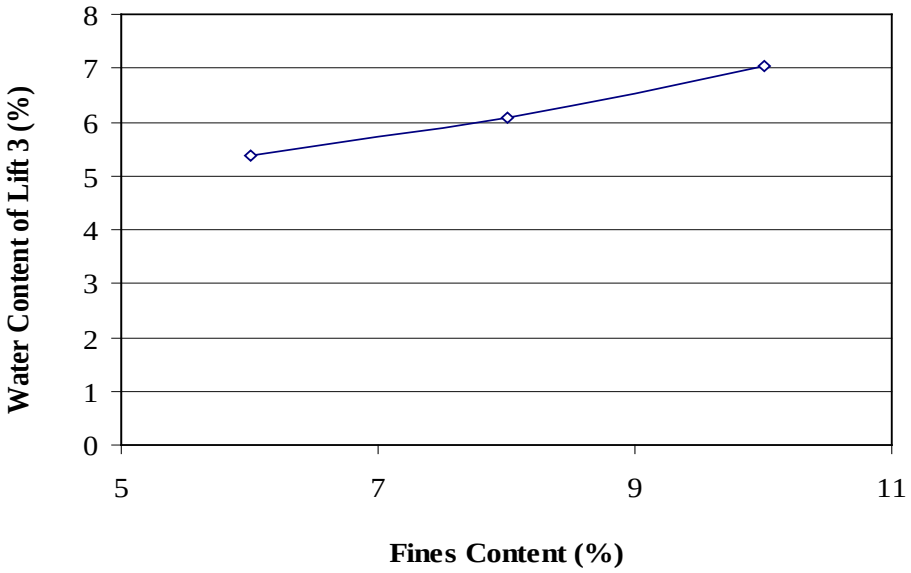

Figure A.10: Main effect of fines content on water content of lift 3.

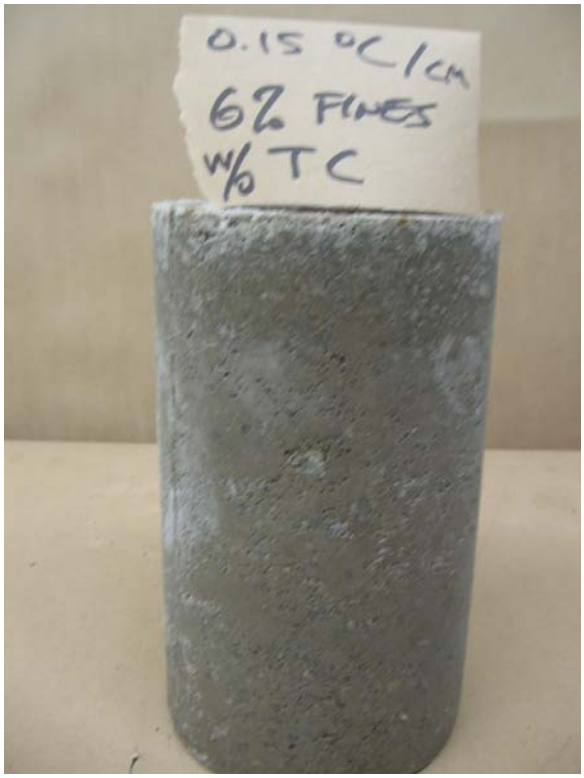

Figure A.11: Specimen with 6 percent fines tested without thermocouples at thermal gradient of 0.15°C/cm.

Figure A.12: Specimen with 6 percent fines tested with thermocouples at thermal gradient of 0.15°C/cm.

Figure A.13: Specimen with 8 percent fines tested without thermocouples at thermal gradient of 0.15°C/cm.

Figure A.14: Specimen with 8 percent fines tested with thermocouples at thermal gradient of 0.15°C/cm.

Figure A.15: Specimen with 10 percent fines tested without thermocouples at thermal gradient of 0.15°C/cm.

Figure A.16: Specimen with 10 percent fines tested with thermocouples at thermal gradient of 0.15°C/cm.

Figure A.17: Specimen with 6 percent fines tested without thermocouples at thermal gradient of 0.30°C/cm

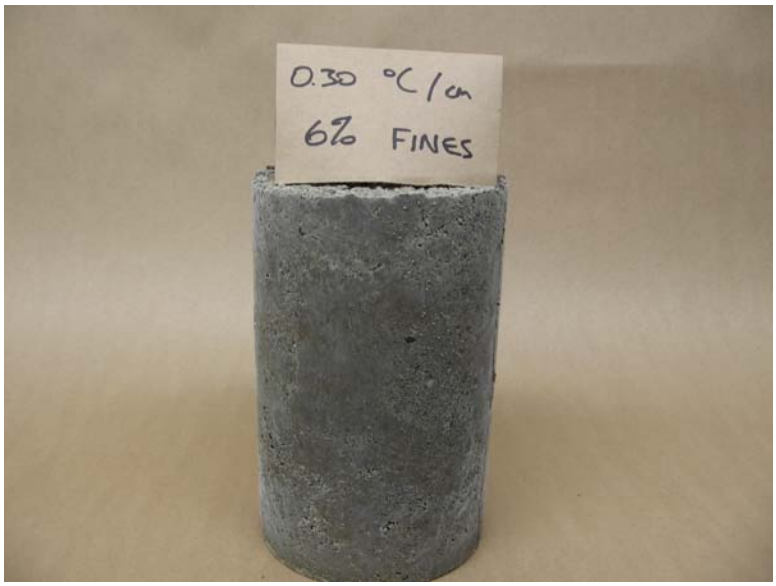

Figure A.18: Specimen with 6 percent fines tested with thermocouples at thermal gradient of 0.30°C/cm

Figure A.19: Specimen with 8 percent fines tested without thermocouples at thermal gradient of 0.30°C/cm

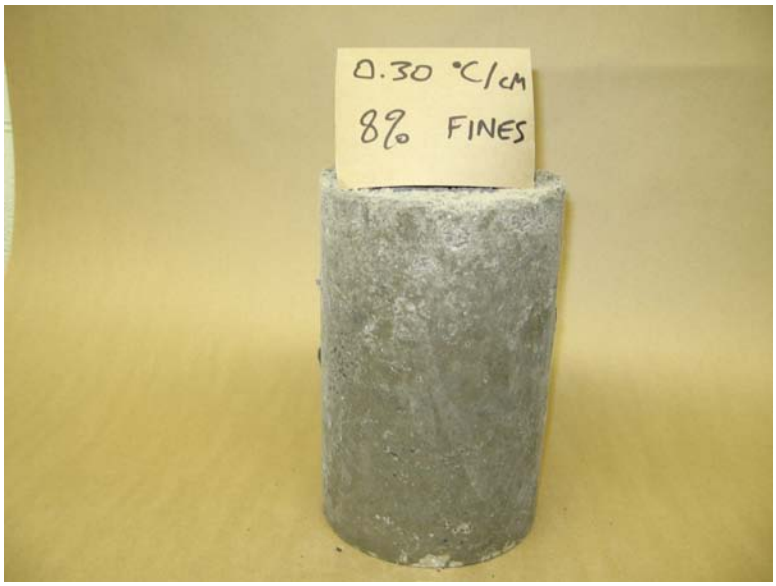

Figure A.20: Specimen with 8 percent fines tested with thermocouples at thermal gradient of 0.30°C/cm.

Figure A.21: Specimen with 10 percent fines tested without thermocouples at thermal gradient of 0.30°C/cm.

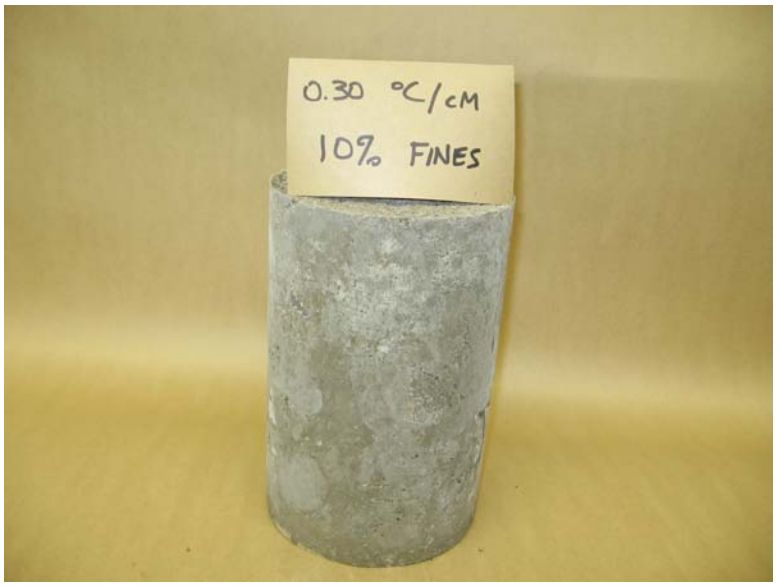

Figure A.22: Specimen with 10 percent fines tested with thermocouples at thermal gradient of 0.30°C/cm.

Figure A.23: Specimen with 6 percent fines tested without thermocouples at thermal gradient of 0.45°C/cm.

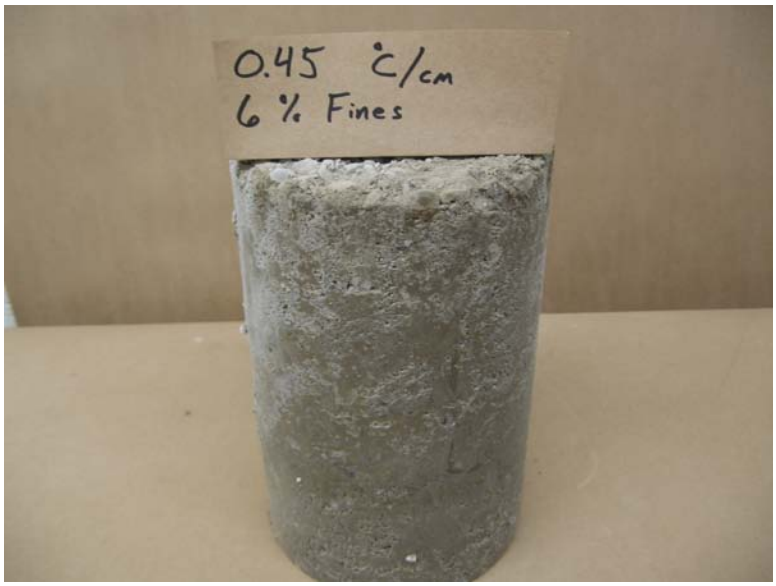

Figure A.24: Specimen with 6 percent fines tested with thermocouples at thermal gradient of 0.45°C/cm.

Figure A.25: Specimen with 8 percent fines tested without thermocouples at thermal gradient of 0.45°C/cm.

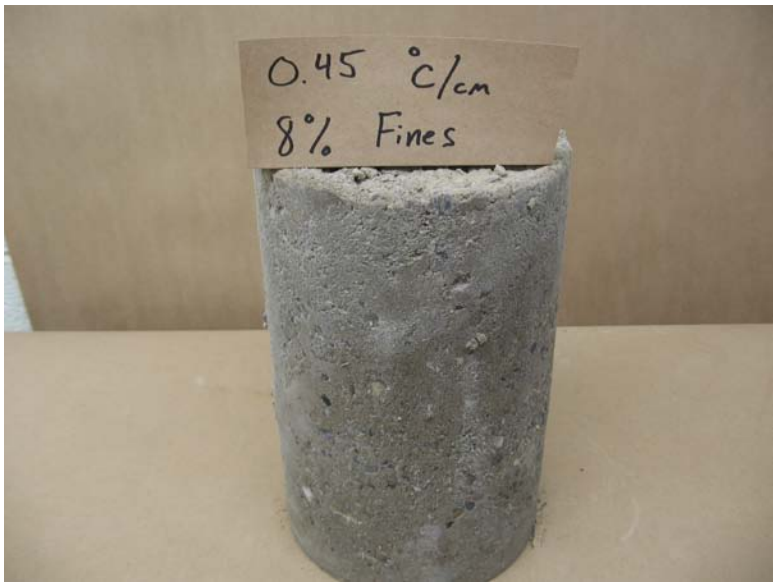

Figure A.26: Specimen with 8 percent fines tested with thermocouples at thermal gradient of 0.45°C/cm.

Figure A.27: Specimen with 10 percent fines tested without thermocouples at thermal gradient of 0.45°C/cm.

Figure A.28: Specimen with 10 percent fines tested with thermocouples at thermal gradient of 0.45°C/cm.